

A novel membrane anchor in the PH-domain is indispensable for dynamin functions

A thesis

submitted in partial fulfillment of the requirements for the degree of

Doctor of Philosophy

by

Himani Khurana

20162003



Indian Institute of Science Education and Research Pune

2023

A novel membrane anchor in the PH-domain is indispensable for dynamin functions

A thesis

submitted in partial fulfillment of the requirements for the degree of
Doctor of Philosophy

विद्या वाचस्पति की उपाधि की अपेक्षाओं की आंशिक पूर्ति में प्रस्तुत शोध प्रबंध

by/ द्वारा

Himani Khurana/ हिमानी खुराना

Registration No./पंजीकरण सं.

20162003

Thesis Supervisor/ शोध प्रबंध पर्यवेक्षक

Prof. Thomas Pucadyil/ प्रो. थॉमस पुकड़ईल



Indian Institute of Science Education and Research Pune


भारतीय विज्ञान शिक्षा एवं अनुसंधान संस्थान पुणे

2023

Certificate

The work incorporated in this thesis entitled ‘**A novel membrane anchor in the PH-domain is indispensable for dynamin functions**’ submitted by **Himani Khurana** was carried out by the candidate under my supervision. The work presented here or any part of it has not been included in any other thesis submitted previously for the award of any degree or diploma from any other University or institution.

In my capacity as the supervisor of the candidate’s thesis, I certify that the above statements are true to the best of my knowledge.


Prof. Thomas Pucadyil

September 18, 2023

Declaration

I declare that this thesis is a presentation of my original ideas and research work, in my own words. Wherever contributions of others are involved, every effort is made to indicate this clearly, with due reference to the literature, adequate citations and acknowledgement of collaborative research as well as discussions. I also declare that I have adhered to all principles of academic honesty, ethics and integrity and that I have not misrepresented, fabricated or falsified any idea/data/fact/source in this submission. I understand that violation of the above will be cause for disciplinary action by the institute and can also evoke penal action from the sources which have thus not been properly cited or from whom proper permission has not been taken when needed. The presented work was carried out under the guidance of Prof. Thomas Pucadyil, at the Indian Institute of Science Education and Research, Pune.



Himani Khurana

September 18, 2023

Dedication

“To my late Grandparents”

Acknowledgements

Science does not happen in a vacuum, and often, there's a troop of thinkers and enablers to thank, for any piece of knowledge ever produced. Here's to mine!

To Thomas Pucadyil, who has been an incredible mentor, and often a friend, *'thank you, for everything!'* It wasn't my farthest of thoughts or ambitions when I first came in, to pursue membrane biochemistry, a dimension of cell biology I was unacquainted with until Thomas's phenomenal work fascinated me. I am deeply grateful that he kindly took me on as a graduate student in all my naivety back then, and directed me to become a self-assured researcher with a whole palette of new found abilities. Every step of the way since, has been a learning experience, with him teaching me pretty much all that I know about the pursuit of science. His *'let's try it out'* approach to challenges, remarkable breadth of knowledge, rooted yet inventive perspective and commitment towards science have been nothing short of inspirational. He has placed a solid foundation in my growth as a scientist with his profound guidance. For that and his untiring support, he holds credit for each little success that I will go on to bag along the way, from here on. I truly appreciate the gamut of perceptive discussions had with him and look forward to carrying these insights with me. I continue to imbibe his adept scientific writing and storytelling skills. His exceptional way with words, with which he most lucidly articulates intricate concepts, is a faculty I almost envy and hope to instill in me someday. For now, I'll say, *'I couldn't have asked for a better mentor, it's been a pleasure working with you, Thomas!'*

I express my sincere thanks to Dr. Anand Srivastava and Krishnakanth Baratam, at the Indian Institute of Science, Bangalore, who I thoroughly enjoyed collaborating with! I'm grateful for the time and effort that Prof. Richa Rikhy and Dr. Amrita Hazra took for my annual talks and for their inputs in research advisory committee discussions during my tenure. Special thanks for the core skills they helped me develop, particularly through briefly working with Richa. Discussions with Prof. Satyajit Rath, Prof. Aurnab Ghose, Dr. Nagaraj Balasubramanian and Dr. Sudha Rajamani have been inspiring. I deeply admire the enriching conversations shared with Dr. Nishad Matange around music, art and science, among other themes!

I thank Pucadyil lab members, both past and present, for frequent enriching discussions. I'm very glad to have overlapped briefly with Srishti Dar, Raunaq Deo, Devika Andhare and Sukrut

Kamerkar who taught me the very alphabets of research, and gave me the first much-needed template of a *how-to-survive-this* guide. I have shared this journey packed with highs and lows, closely with Soumya Bhattacharyya and Krishnendu Roy who pushed me to do better in their own ways. I acknowledge Soumya's help with a piece of this project, the data produced from which is included in *Chapter 7* of this thesis. Uma Swaminathan, Shilpa Gopan, Raksha Bhansali, Meghadeepa Sarkar, Keerti Singh, Sannidhya De, Gurmail Singh, Aman Sharma and Swayam Singh have been fun to work with and supportive through the daily hustle. Gregor Jose, Rakhee Lohia, Prasanna Iyer, and Parul Sood, the few postdocs I happened to work along, even if briefly, have been delightful and encouraging. I'm grateful for all joyful and drab times shared with all these people, who assured to liven things up, once in every while!

I admire the common lab environment at IISER Pune that enables swift resource sharing and fosters collaboration among peers! I must also acknowledge IISER Pune's hardworking and excellent support staff in the research and upkeep facilities such as microscopy, proteomics, cell culture, cell sorting, bio-office, maintenance & repairs, security, administration and housekeeping. I'd like to acknowledge financial assistance from IISER Pune and HHMI foundation for research fellowships, and HHMI foundation, EMBO and SERB-ITS for generous travel awards that assisted me to present my work internationally.

To my family, for their unyielding faith in me and unconditional support, '*thank you!*'. All my triumphs are rooted in the values that *maa* and *paa*, Anjula and Vinod Khurana instilled in me. I ought to thank my *maasi* - Dr. Geeta Rani who has a formative role in my academic training as I learnt the first lessons in research during school, while helping put together her graduate work. The insistent care she and my *chachu*, Mr. Bharat Bhushan Khurana nurtured me with, had me believe I could achieve anything I put my mind to. It would be apt to say I was raised by four parents. I have my brother Mukul and adorable sisters Naaz and Jiaa Khurana to thank, for pulling me back home every so often, and spoiling me silly with pure affection. Heartfelt thanks to my brother for being close to home so I could be far without a worry, and for taking the occasional uplifting drives with me which I hold very dear!

This erratic ride full of ups & downs has been survived by my friends. Gauri Binayak, Aparna Sundaresan, and Kaveri Vaidya have always had my back. I got through the roughest days with much ease, with them by my side. I will always adore all the reveries, debates and silences we shared. I owe special thanks to GB for being my person on my happiest and most dreary days.

I'm grateful for all the blitheness shared with my batchmates that almost never let monotony set in. I dearly thank Rahul Biradar for always being my biggest cheerleader, even from across continents. I hold immense gratitude for Shivani Bodas, with whom, years felt like days as she had me smiling through the good, bad and ugly. I'm grateful to have found in her a confidant, and a commendable partner in all things; and am pleased she made me comfortable with furry friends who are now a vital part of my life. *'There was never a dull moment around you and am overjoyed that our paths crossed!'* This note is incomplete without affirming the unwavering support that Suyash Naik rendered through the years by becoming my best critic, constant sounding board, and anchor. I couldn't confine to words the sundry ways in which this friendship has indelibly molded me but I'll say this much, *'often, your mere presence and sheer verve carried a semblance of peace making the hardest times seem fleeting.'* I owe him a special thanks for proofreading pretty much everything I wrote, and urging me to learn to code, which became surprisingly resourceful. I'm evermore indebted to him for incessantly propelling me to shoot for the stars!

In all, this has been a humbling and heartening journey. I formed a few lasting friendships along the road, some memories I will cherish and lessons I will carry. Gratefully, life here, at the edge of hills and city, blended quiet and alive impeccably. Gradually indeed, I knit the tightest fall back in my recouped knacks to paint abstractly, strum the strings, read ardently, thread musings in words, and practice yoga; that kept me sane through the bleakest hours.

'So Long, and Thanks for All the Tea & Coffee!'^

*^adapted from 'The Hitchhiker's Guide to the Galaxy' trilogy, books by Douglas Noël Adams.
"...& somewhere in between galaxies of neurons and narratives; we keep on, keeping on!"*

Table of Contents

Abstract	01
Synopsis	02
List of figures	05
Chapter 1. Introduction	07
1.1 Intracellular organisation and membrane traffic in eukaryotic cells	08
1.2 Membrane remodeling is central to membrane traffic	10
1.3 A glance at dynamin superfamily in membrane-active cellular processes	11
1.4 Classical dynamins as paradigmatic membrane fission catalysts	12
1.5 Mechanistic view of the mechanochemical molecular scissor: Dynamin	14
1.6 Membrane-interacting ‘variable loops’ in the PH-domain	16
1.7 The effector role of PH-domain (PHD) in dynamin function	17
1.8 Dynamin-PHD as a hub of congenital neuropathy & myopathy linked mutations	18
1.9 Key findings from molecular dynamics simulations and structural modeling	20
Chapter 2. Materials and methods	23
2.1 Constructs, cloning, and plasmids	23
2.2 Protein-expression, purification and fluorescent labelling	23
2.3 Liposome preparation	25
2.4 GTPase activity assays	26
2.5 Liposome co-sedimentation assay	26
2.6 Proximity-based labelling of membrane associated proteins (PLiMAP)	27
2.7 Supported membrane templates (SMrT) preparation, assays and analysis	28
2.8 Cell culture and transferrin-uptake assay	29
2.9 Fluorescence imaging and image analysis	30
Chapter 3. Brief rationale: A prelude to the results	31
Chapter 4. Probing dynamin functions on highly anionic membranes	34
4.1 The variable loops (VLs) in dynamin PHD are highly conserved regions	35
4.2 Testing a VL4 tip mutant with reduced hydrophobicity - Dynamin1 F579A	36
4.2.1 GTP-hydrolysis activity	37

4.2.2	<i>Membrane binding</i>	37
4.2.3	<i>Membrane fission using Supported Membrane Templates</i>	38
4.3	Discussion	39
Chapter 5.	Probing the significance of the novel VL4 in dynamin-mediated fission on membranes of physiological phospholipid composition	40
5.1	Dynamin1 F579A shows reduced membrane binding affinity in bulk assays	41
5.2	Dynamin1 VL4 tip mutants with perturbed loop hydrophobicity show curvature sensitive defects in membrane binding and self-assembly	42
5.3	Dynamin1 VL4 tip mutants with reduced loop hydrophobicity but not altered loop charge, show curvature sensitive defects in membrane fission	44
5.4	Dynamin2 functions are more sensitive to membrane curvature than Dynamin1	44
5.5	Discussion	45
Chapter 6.	Comparative analysis of variable loop effects on dynamin functions	47
6.1	Membrane fluorescence correlated to tube radius enables study of intermediates formed during real-time analysis of dynamin-catalysed membrane fission	49
6.2	VL4 facilitates whereas VL1 inhibits dynamin-mediated membrane fission	50
6.3	Discussion	51
Chapter 7.	Reconstituting dynamin functions in a native-like context	52
7.1	A dynamin binding partner BIN1 (Amphiphysin2) is membrane-active	53
7.2	BIN1 recruits both Dynamin1 and Dynamin1 F579A to membrane nanotubes	55
7.3	Dynamin1 F579A shows dramatic lack of fission on BIN1 coated-tubes	56
7.4	Discussion	57
Chapter 8.	Probing the significance of VL4 in cellular functions of dynamin	59
8.1	Dynamin1 F579A and M580T impair clathrin-mediated endocytosis in cells	60
8.2	Discussion	62
Chapter 9.	Summary, discussion and perspectives	63
	Publications and permissions	71
	References	73

Abstract

A novel membrane anchor in the PH-domain is indispensable for dynamin functions

A host of dynamin superfamily proteins undertake diverse membrane-active processes in cells. Classical dynamins are paradigmatic membrane fission catalysts that release vesicles by acting on the neck of nascent endocytic buds during clathrin-mediated endocytosis (CME). Notably, among fission dynamins, endocytic dynamins have evolved a specialized membrane-binding *pleckstrin-homology domain* (PHD). PHD facilitates dynamin-mediated membrane fission catalytically, but the underlying mechanism is unclear. PHD-membrane interaction occurs via hydrophobic and basic residues enriched in the highly conserved unstructured ‘variable loops’ (VLs). Literature identifies dynamin PHD as a hotspot for pathological mutations associated with congenital neuropathy and myopathy. Molecular dynamics (MD) simulations and structural modeling recently reported a novel loop *viz.* VL4 as a preferred membrane anchor after the previously known VL1, whose relevance in dynamin function remains unexplored. To this end, we perform a suite of biochemical and cellular assays and mechanistically link *in silico* data to physiology. In minimal lipid-based recruitment assays, we find that mutations perturbing VL4 hydrophobic character manifest partial defects in membrane binding and fission. Fine real-time analysis establishes discrete and separable effects of VL1 and VL4 in dynamin-mediated membrane fission. Remarkably, more native-like reconstitution involving lipid and protein interactions reveals a complete loss in fission despite dynamin being effectively captured on the membrane, signifying an active contribution of the PHD in membrane fission. Importantly, expression of VL4 mutants in cells inhibit CME, consistent with the autosomal dominant phenotype associated with VL4-linked Charcot-Marie-Tooth neuropathy. These results bring out the basis of catalytic contribution of PHD in dynamin function and emphasize the significance of finely tuned lipid and protein interactions for efficient vesicle release by dynamin.

Synopsis

A phospholipid bilayer of approximately five nanometer thickness delimits all cellular and organellar membranes. This perimeter is resilient to rupture but is frequently breached in the event of vesicle formation. Cells have evolved dedicated protein machinery to actively drive this thermodynamically unfavorable process of membrane bending and fission.

Dynamin is the prototypical membrane fission catalyst that forms helical collars around the neck of nascent coated-buds and utilizes GTP-hydrolysis assisted conformational changes to bring about progressive constriction and subsequent fission of the underlying membrane bilayer facilitating vesicle release during clathrin-mediated endocytosis or CME. The large GTPase dynamin harbors a multi-domain module attributing various functional facets to the molecule. It has an amino-terminal *G-domain* responsible for GTP-binding and hydrolysis, a *four-helix bundle 'stalk'* that promotes self-assembly; a *pleckstrin-homology domain* (PHD) that interacts with phospholipids, a *three-helix 'bundle signaling element'* (BSE) wherein three independent alpha helices otherwise distant in the primary sequence come together in the folded monomer. In its folded state, the G-domain depicts the head, BSE is the neck, the stalk forms the trunk and the PH-domain forms the foot of the molecule. The BSE relays significant conformation switches realized upon GTP-hydrolysis from the G-domain through the molecule. These traverse as mechanical forces actively aiding membrane fission. Finally, an unstructured carboxy-terminal *proline rich domain* (PRD) in dynamin is seen that binds SH3 domain-containing proteins by virtue of which cytosolic dynamin is captured at the neck of nascent clathrin-coated pits towards later stages of clathrin-mediated endocytosis.

Among the diverse dynamin superfamily, classical or endocytic dynamins have evolved a dedicated *pleckstrin-homology domain* (PHD) for membrane anchoring as opposed to an unstructured stretch seen in ancestral dynamin-related proteins. Neurons predominantly express dynamin1 of the classical dynamins that mediates the swift release of clathrin-coated vesicles during synaptic vesicle recycling. The dynamin PH-domain or PHD has been shown to have preferential affinity for phosphatidyl inositol (4,5) bisphosphate *viz.* PI(4,5)P₂ or PIP₂, rich in the plasma membrane's inner leaflet, largely governed by precise electrostatic interactions. The PH-domain core consists of two anti-parallelly oriented beta-sheets and a carboxy-terminal alpha helix, built from just over a hundred residues. Consecutive beta strands are connected via unstructured loops called variable loops. Only three variable loops (VL1-3) have been annotated for the dynamin PHD in literature. Various studies have established that

VLs are indispensable for optimal dynamin function. Isoleucine (I533) of VL1 in the dynamin1 PHD has been shown to wedge into the membrane bilayer owing to its hydrophobic character. VL2 and VL3 are better known for electrostatic interactions with anionic phospholipid headgroups due to their relatively polar, mostly basic character.

Recent study aimed at understanding PHD-membrane engagement has annotated a novel variable loop (VL4) of seven residues stretching across 576-582 positions in human dynamin1. The study also demonstrates using atomistic molecular dynamics simulations that the novel VL4 comes in very close proximity of the underlying bilayer, as is known for VL1. The relevance of this interaction is not at all understood for dynamin function as in the simulations, the dynamics are recorded within a restricted framework of an isolated dynamin1 PHD on a planar phospholipid-bilayer. This study also reports that variable loop insertion in the bilayer lowers membrane bending rigidity making it more pliable for fission. This goes on to expand the understanding of the mechanism of dynamin-mediated membrane fission from the perspective of biophysical changes experienced by the membrane.

PHD function in dynamin seem to extend beyond membrane-binding. Stalk binding, for instance, is one such aspect of PHD-function, which holds dynamin in an autoinhibitory state and impedes self-assembly in solution. Moreover, it has been demonstrated in a previous study from the lab using minimal systems that PHD is dispensable for dynamin-mediated membrane fission but appears to contribute catalytically to the fission process. Importantly, mutations in the dynamin PHD are often linked to neurological disorders such as centronuclear myopathy (CNM) and Charcot-Marie-Tooth (CMT) neuropathy. In fact, a genetic study reported dynamin2 *Met580Thr* as a pathological mutation found in an autosomal dominant form of CMT. Notably, this missense mutation lies at the tip of the newly annotated VL4 region in the dynamin PHD, whose relevance to dynamin function remains completely unexplored. Interestingly, MD simulations with VL4 mutants that perturb VL4 hydrophobicity showed no apparent defects. These contrasting aspects encouraged us to experimentally probe the significance of VL4 in dynamin function and dissect the general molecular basis of the catalytic activity of PHD in dynamin-mediated membrane fission.

Chapter 1 of this thesis provides a comprehensive introduction describing how active membrane remodeling is central to vesicle traffic and overall organization of eukaryotic cells. It goes on to elaborate the known intricacies of dynamin superfamily proteins finally leading up to a detailed molecular picture of role of PH-domain in dynamin-mediated membrane fission during clathrin-mediated endocytosis.

Chapter 2 contains an elaborately put together account of all the methods, data collection and data analysis performed during the course of this study. The description also entails specifics of commercial and non-commercial sources for all reagents used along with the vendor and catalog details.

Chapter 3 provides a brief rationale logically connecting the previously described literature in the introduction section to the motivation for the present research, forming a prelude to the results of the present study, discussed in the following chapters.

Chapter 4 discusses results from assays that are aimed at validating the mutant constructs of dynamin generated for this work, in terms of proper folding, GTP-hydrolysis activity, membrane-binding as well as membrane fission. The assays described in this chapter are all performed on membranes displaying high anionic character whose physiological relevance is implausible. However, these membranes are appropriate for testing global defects in dynamin functions as they are not limiting in the substrate i.e., negatively charged lipids.

Chapter 5 attempts to bring-out a much finer analysis of dynamin functions upon perturbation of VL4 hydrophobicity using membranes that exhibit physiological lipid composition via bulk (liposome-based) as well as fluorescence microscopy-based assays.

Chapter 6 describes in precise detail, the differential effects of variable loop membrane insertion on dynamin functions by performing a comparative analysis of intermediates observed during dynamin-mediated membrane fission with VL1 & VL4 mutants.

Chapter 7 entails a discussion of results from assays that attempt to reconstitute dynamin functions in a much more native-like context by using both protein and lipid-based bivalent interactions in the assays that closely mimic cellular dynamin interactome, as opposed to results described in chapter 5 where dynamin-membrane recruitment is solely lipid-based.

Chapter 8 finally uncovers findings from assays monitoring the internalisation of transferrin, the canonical CME cargo, upon expression of VL4 mutants with reduced hydrophobic character in live cells in order to examine their efficiency at mediating vesicle release during clathrin-mediated endocytosis, in the intricate and regulated cellular milieu.

Chapter 9 contains a brief summary of the findings described in the preceding chapters, a thorough discussion of our results in the context of the existing literature highlighting how this study propels our understanding of dynamin-mediated membrane fission by leaps and bounds, and eventually a few intriguing facts and future perspectives about the unexplored abundant diversity of various pleckstrin-homology domains encoded in the human proteome.

List of figures

Chapter 1. Introduction

<i>Figure 1.1</i>	Schematic depicting membrane traffic in eukaryotic cells	09
<i>Figure 1.2</i>	Schematic depicting the cascade of events in clathrin-mediated endocytosis	10
<i>Figure 1.3</i>	Dynamin domain architecture and dimer structure in solution	12
<i>Figure 1.4</i>	Comparison of domain architecture in endocytic versus ancestral dynamins	15
<i>Figure 1.5</i>	Structure of the dynamin pleckstrin-homology domain	17
<i>Figure 1.6</i>	Dynamin domain architecture highlighting disease-linked mutations	19
<i>Figure 1.7</i>	Variable loops in the dynamin pleckstrin-homology domain	20

Chapter 2. Materials and methods

<i>Figure 2.1</i>	Schematic depicting the workflow of a liposome co-sedimentation assay	27
<i>Figure 2.2</i>	Schematic depicting the workflow of a PLiMAP assay	27
<i>Figure 2.3</i>	Schematic depicting supported membrane templates' preparation workflow	28
<i>Figure 2.4</i>	Schematic depicting a transferrin uptake assay	30

Chapter 3. Brief rationale: A prelude to the results

<i>Figure 3.1</i>	Surface rendered structural model of a dynamin polymer	33
-------------------	--	----

Chapter 4. Probing dynamin functions on highly anionic membranes

<i>Figure 4.1</i>	Sequence alignment of dynamin pleckstrin-homology domain	35
<i>Figure 4.2</i>	Surface rendered model of dynamin PHD highlighting charge distribution	36
<i>Figure 4.3</i>	Dyn1 membrane binding and GTP hydrolysis on highly anionic membranes	38
<i>Figure 4.4</i>	Dynamin mediated membrane fission on highly anionic membranes	39

Chapter 5. Probing the significance of the novel VL4 in dynamin-mediated fission on membranes of physiological phospholipid composition

<i>Figure 5.1</i>	Dynamin binding analysed on physiological membranes in bulk assays	41
<i>Figure 5.2</i>	Dynamin binding to physiological membranes in microscopic assays	43
<i>Figure 5.3</i>	Comparative analysis of Dyn1/2 fission activity on physiological membranes	45

Chapter 6. Comparative analysis of variable loop effects on dynamin functions

Figure 6.1 Dynamin1 scaffold constrict the underlying membrane tube ----- 48

Figure 6.2 Dynamin1 self-assembly and GTPase induced constriction leading to fission _ 51

Chapter 7. Reconstituting dynamin functions in a native-like context

Figure 7.1 BIN1 or Amphiphysin2 is membrane active ----- 54

Figure 7.2 BIN1 scaffolds stably recruit Dyn1 F579A on the membrane ----- 55

Figure 7.3 Dyn1 F579A is incapable of inducing fission of BIN1-coated tubes ----- 57

Chapter 8. Probing the significance of VL4 in cellular functions of dynamin

Figure 8.1 Assaying cellular functions of dynamin by estimating transferrin-uptake ---- 61

Chapter 1

INTRODUCTION

1.0 Introduction

Membranes are indispensable for all life forms. Cellular membranes are formed by amphipathic building blocks *viz.* phospholipids that spontaneously self-assemble into a five nanometer-thin bilayer in aqueous environments. Being semi-permeable, these membranes allow only selective passage-way across their boundaries. These properties perhaps lie at the heart of phospholipids being selected as materials to contain biochemical reactions that functionalize cells and birth life. Membranes do act as barriers that serve to concentrate biochemical reactions within a delimited space. In addition to that, chemical diversity in cellular phospholipids actively shapes crucial molecular networks. Such confinement of biochemical reactions enables active regulation of cellular functions in space and time. The membrane surface therefore forms a fundamental platform upon which a multitude of processes that are central to cellular homeostasis are actively choreographed¹.

1.1 *Intracellular organisation and vesicle traffic in eukaryotic cells*

The compartmentalization of the cytoplasm by membrane-bound organelles is a hallmark of eukaryotic cells. Membrane chemistry at various compartments directs downstream signalling thereby shaping all molecular networks and communication within and across cells². Intracellular organelles display distinct combinations of proteins and lipids that define their biochemical identity, form and function.

Phospholipid and protein synthesis occurs in the endoplasmic reticulum (ER) from where these are delivered to destined compartments by active sorting pathways. Lipid modulating enzymes localised differentially across intracellular membranes provide local phospholipid turnover generating phospholipid gradients and biochemical signals, but all organelles rely on the ER for precursor phospholipid supply³. Lipid and protein transport across the cytoplasm predominantly occurs through ‘membrane traffic’ wherein a portion of an existing donor organelle is pinched off as a membrane-bound vesicle or tubule packed with specific luminal and membrane-associated cargo, and then transferred to an acceptor organelle (Figure 1.1). This governs the distribution of lipids and proteins in a spatiotemporally regulated manner. Importantly, *membrane traffic or vesicle traffic* coordinates intra- and inter-cellular communication by shaping the signalling landscape underlying processes such as nutrient uptake, secretion, cell-adhesion, cell-migration, and cell-division. Any perturbation of lipid-protein homeostasis is linked with a myriad of metabolic and neurodegenerative disorders.

Membrane trafficking is a key phenomenon that directs the intracellular flux of lipids and proteins synthesized in the ER. Since the first electron micrographs of a cell that shed light on intracellular organization⁴, persistent meticulous advances in electron and fluorescence microscopy and live-cell imaging have disclosed ultrastructure and dynamics of the endomembrane system i.e., the plasma membrane, endoplasmic reticulum, golgi apparatus, and the endo-lysosomal compartments⁵⁻⁷. After the discovery of vesicles as a means of exchange between organelles by George Emil Palade⁸ and colleagues in the 1970s, an abundance of information from seminal biochemical, genetic and cellular studies has produced a detailed picture of the molecular networks that orchestrate vesicle traffic. This distinguished secretory and endocytic pathways determining cargo flow and vesicle flux through the anterograde (ER to golgi to plasma membrane) and retrograde routes (plasma membrane to endosomes or golgi to ER) of vesicle transport and revealed that each event of vesicle formation is sustained by coordination of hundreds of different proteins⁹⁻¹⁷.

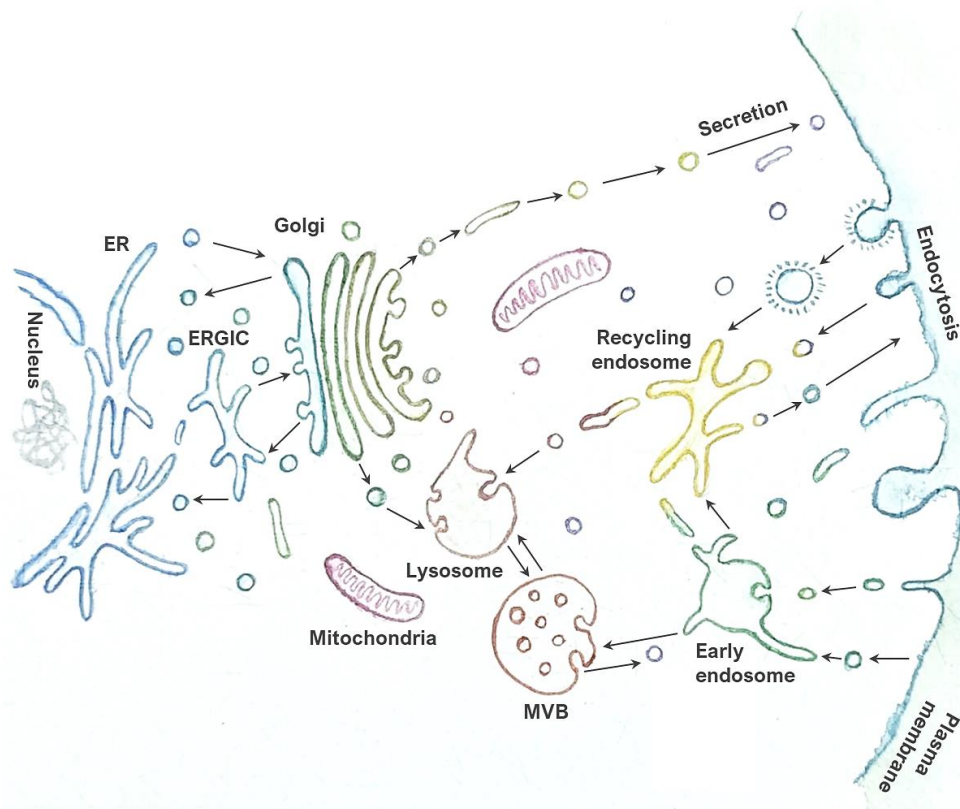


Figure 1.1 Schematic depicting membrane traffic in eukaryotic cells.

Key pathways in membrane traffic across compartments of the endomembrane system within eukaryotic cells. Colors signify biochemically & morphologically distinct compartments that exchange vesicular or tubular carriers concentrated with demixed cargoes. Abbreviations as follows, ER: Endoplasmic reticulum, ERGIC: ER-golgi intermediate compartment, MVB: multivesicular body (or the late endosome). Arrows signify various routes and direction of flux.

1.2 Membrane remodeling is central to membrane traffic

Phospholipid membranes that delimit cells and membrane-bound organelles are resilient to rupture. Yet, this perimeter is frequently breached in the event of vesicle formation as cells have evolved active mechanisms to drive this thermodynamically unfavourable process by membrane-active proteins that manage key steps in vesicle formation i.e., membrane bending, fission and fusion^{11,12}. While some vesicles contain coat-proteins (such as clathrin-coated vesicles from plasma membrane or coat protein complex I or II (COPI or COPII) coated vesicles from golgi or the ER respectively) that induce or stabilize high membrane curvature during vesicle budding, several vesicles exchanged among the endosomal and lysosomal compartments are apparently devoid of such coats^{11,18,19,12,20,21}.

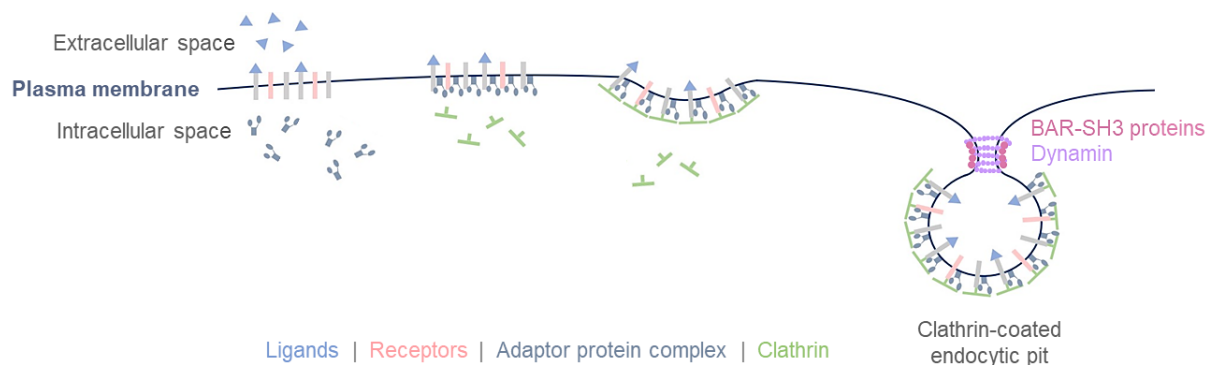


Figure 1.2 Schematic depicting the cascade of events in clathrin-mediated endocytosis.

During clathrin-mediated endocytosis, membrane curvature is initiated by engagement of adaptor proteins, cargo receptors, membrane phospholipids and clathrin polymerization. During the later stages, BAR domain scaffolds induce a tubular neck topology and SH3 domains capture cytosolic dynamin at the neck where it forms helical collars, and catalyses membrane fission by GTPase induced constriction to mediate vesicle release.

Clathrin-mediated endocytosis (CME) is one of the most well characterized pathways of vesicle formation^{22,23}. During CME, the coat-protein clathrin along with several adaptor proteins, accessory proteins and BAR (Bin-Amphiphysin-Rvs) domain-containing proteins builds the coated-vesicle. During early stages, dedicated adaptor i.e., adaptor-protein complex 2 (AP2) recognizes cargo and PI(4,5)P₂ or PIP₂ in the inner leaflet of the plasma membrane and recruits clathrin on the endocytic site^{24,25}. This nucleates clathrin polymerisation in a basket-like structure built by clathrin triskelia forming hexagonal lattices, which proceeds while resculpting the membrane underneath it and birthing a clathrin-coated pit (CCP)²⁶. This

nascent bud matures as clathrin polymerises in about a minute and concentrates the cargo within its perimeter by virtue of protein-protein interactions. During the later stages of pit maturation, scaffolding proteins such as BAR domain-containing proteins are recruited to the neck where they induce curvature and define a tubular intermediate that eventually undergoes scission by dynamin, a large mechanochemical GTPase, belonging to the dynamin superfamily of proteins²⁷⁻³³.

1.3 A glance at dynamin superfamily in membrane-active cellular processes

Genetic screens along with biochemical and structural studies have led to identification of a variety of membrane-active proteins among which several dynamin superfamily proteins (DSPs) feature³⁴. The dynamin superfamily is an assortment of multidomain large GTPases that are known for their roles in various membrane-active processes from prokaryotes to higher eukaryotes³⁵. DSPs are GTP-hydrolysing enzymes with a structurally conserved mechanochemical core. Each DSP has a minimal module built of a globular G-domain and a helical bundle or 'stalk'. The G-domain generates chemical energy by GTP-hydrolysis and transforms this into mechanical energy in the form of relayed conformational shifts during the hydrolysis cycle. The stalk is a helical bundle with interfaces for self-assembly that determine formation of higher-order oligomers^{36,37}. Over the course of evolution, various DSPs have evolved additional domains for specialised functions. A number of dynamin superfamily proteins across evolution have been classified into membrane fission, fusion and scaffolding proteins³⁸. Bacterial dynamin-like proteins (BDLP); yeast vacuolar-protein sorting protein (Vps1), yeast dynamin-like protein (Dnm1-2); and mammalian dynamins such as classical dynamins (Dyn1-3) and dynamin-related protein1 (Drp1) have been ascribed specialised membrane fission roles during different cellular processes³⁸⁻⁴¹. DSPs Drp2-5, that are closest relatives of the mammalian dynamin-related protein Drp1, are linked to membrane-active roles in plant cells³⁸. Eukaryotic dynamin superfamily members such as Opa1, mitofusins, and atlastins (yeast Mgm1, Fzo1 and Sey1) have reported roles in membrane association and fusion at various cellular membranes^{42,43}. Mammalian Eps15 homology (EH) domain-containing proteins (EHD1-4) have been associated with membrane tubulation and fission at endosomal compartments^{44,45}. Mammalian DSPs *viz.* Mx proteins and guanylate-binding proteins (GBPs) are scaffolding proteins that confer viral resistance⁴⁶. Together, dynamin superfamily members support numerous processes including pinching-off transport vesicles; protein dispersal, recycling and degradation; division of organelles, maintenance of organelle morphology;

cytokinesis and pathogen resistance within cells^{34,38}. They also govern display of cell-surface proteins and in-turn affect cell-cell communication, cell-adhesion and migration making them key regulators of fundamental cellular processes. In humans, disrupted DSP function is linked with numerous physiological disorders.

1.4 Classical dynamins as paradigmatic membrane fission catalysts

Building the membrane fission catalyst - Dynamin

In addition to the core DSP domains specialised lipid-protein interaction domains have evolved in classical dynamins⁴⁷. Each dynamin monomer comprises of five domains contributing to its multi-faceted function enabling nucleotide hydrolysis, membrane binding, self-assembly and multimeric protein interaction that work in concert to achieve membrane fission⁴⁷⁻⁵¹. Among these, a dynamin monomer exhibits four structural components, which can be conceptualized as the head, neck, trunk, and foot segments of the molecule^{41,52} (Figure 1.3). The fifth region is however an unstructured stretch at its carboxy-terminus called the proline-rich region (PRR) or proline-rich domain (PRD). The head constitutes a globular G-domain, while the trunk consists of a four-helix bundle known as the ‘stalk’ domain. Connecting the head to the trunk is the neck, which forms a three-helix bundle functioning as a bundle signalling element (BSE). The molecule's foot is a pleckstrin-homology domain (PHD) responsible for membrane binding. The C-terminal PRD remains unstructured in solution and is therefore deleted in several reported dynamin structures⁵³⁻⁵⁵.

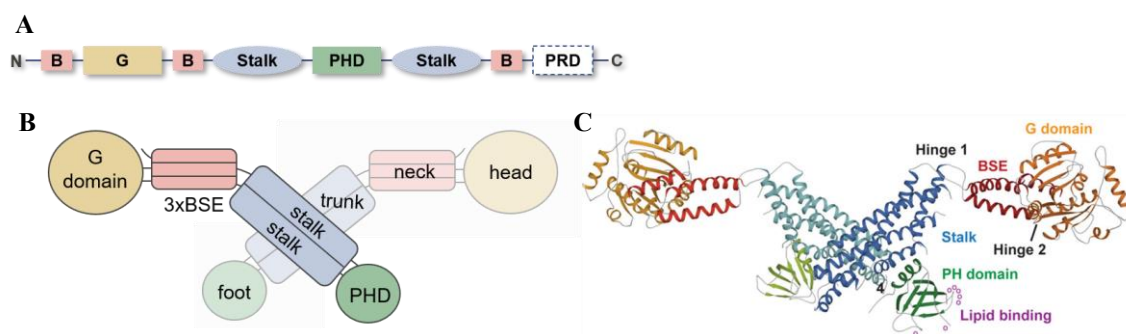


Figure 1.3 Dynamin domain architecture and dimer structure in solution.

A. Primary sequence and dynamins domains. Each domain is colour coded consistently in the entire figure to highlight composite elements in the folded structure. **B.** Block diagram of a dynamin dimer, defining the head, neck, trunk, and foot of the molecule in the faded monomer, complementary to the respective domains shown in the brighter monomer. **C.** Crystal structure of a dynamin dimer, reproduced from reference⁴⁸.

Functions of classical dynamins (cDyn) are best characterized in the context of vesicle release by membrane fission during clathrin-mediated endocytosis (CME) therefore, they're also called endocytic dynamins⁵⁶. During clathrin-mediated endocytosis (CME), a coordinated cascade of interactions between proteins and lipids leads to the formation of small bud-like structures called clathrin-coated pits (CCPs) on the inner leaflet of the cell membrane. As these nascent coated-pits mature, they accumulate the coat-protein clathrin that polymerises in basket-like hexagonal lattices imposed on the bud periphery^{28,33}. At the edge where these buds are connected to the plasma-membrane, CCPs recruit BAR-domains that induce curvature and form the narrow tube-like neck of the pits (Figure 1.2). These BAR domain-containing proteins such as amphiphysin, endophilin, syndapin etc. directly associate with the C-terminal PRD of dynamin via their Src-homology3 (SH3) domains and capture cytosolic dynamin at the tubular neck of nascent clathrin coated-pits^{57,58}. Such protein-protein interactions drive cytosolic dynamin to its site of action before it engages with the membrane.

Classical Dynamins: Similar yet Different

There are three dynamin paralogs encoded in the mammalian genome, each with distinct functions and tissue expressions^{59,60,49}. Dynamin1 of the classical dynamins is predominantly a cytosolic protein abundantly expressed in neurons that mediates the release of clathrin-coated vesicles during fast synaptic-vesicle recycling²⁶. Dynamin2 is a ubiquitously expressed paralog that manages bulk CME in cells, and dynamin3 is expressed in neurons in small amounts and plays a role in various membrane remodeling processes such as maintenance of dendrite morphology⁶¹⁻⁶⁵. Recent studies have also established a connection between dynamin1's fission activity and the regulation of synaptic vesicle size⁶⁶.

These dynamin types differ subtly in their ability to enzymatically break down GTP and remodel membranes. Dynamin1 exhibits the highest stimulation in GTPase activity upon self-assemble on membranes. It also binds to and efficiently severs tubes spanning a broad range of curvatures, accomplishing fission activity notably faster than dynamin2⁶⁷. In contrast, dynamin2 shows more curvature sensitivity driving scission of notably thinner tubes and displays a lower level of stimulated GTPase activity. While studies defining the most dissimilar paralog dynamin3's biochemical characteristics are not as extensive, it has been reported that dynamin3 is capable of maintaining the viability of mouse embryonic cells with double knockouts of dynamin1 and dynamin2^{68,69}. This suggests a functional resemblance and at least partial redundancy between dynamin3 and dynamin1/2 activities.

By virtue of having similar core domains, all three dynamin types likely achieve membrane fission using a similar mechanism. However, dynamin 1/2/3 functions are restricted to different sub-cellular locations even in cell types where all three isoforms are expressed. This is likely achieved by means of different partner-protein interactions with the C-terminal proline rich region of dynamin, as it is the least conserved, most disparate region among dynamin paralogs. Therefore, the region serves as a critical platform for regulation of differential dynamin function by directing them to different cellular locations and engaging with different partner-proteins leading to distinct emergent functions^{70,71}.

In addition to differential expression and protein-protein interactions driving tissue-level and subcellular regulation of dynamin function⁷², various signalling axes altering phosphorylation status of the protein or affecting downstream protein interactions also regulate dynamin functions⁷³. In addition, several splice variants of the dynamin paralogs have also been reported that form another axis of differential regulation of dynamin functions in the cell. For instance, recently, functionally distinct splice isoforms of dynamin1, characterized as short and long variants, have been demonstrated to exhibit a particular preference for recruitment and subsequent clustering at sites of endocytosis on the plasma membrane⁷⁴. The process of phosphorylation and dephosphorylation at unique sites within the C-terminal region of the neuronal dynamin1 isoforms, Dyn1xa (long) and Dyn1xb (short), is believed to actively control activity-dependent bulk endocytosis. Additionally, it has recently been reported that the long Dyn1xa isoform tends to associate with Syndapin1 condensates at the synapse, participating in the rapid process of endocytosis⁷⁵.

1.5 Mechanistic view of the mechanochemical molecular scissor: Dynamin

Dynamin is a mechanochemical enzyme that self-assembles to form helical collars on the neck of the clathrin-coated buds and using energy produced from GTP-hydrolysis this scaffold undergoes concerted conformational changes that aid in driving constriction and scission of the underlying membrane, thereby releasing the vesicle⁷⁶⁻⁸¹. Interestingly, among fission dynamins that peripherally associate with membranes, the more primitive design of the mechanochemical enzyme in ancestral dynamins (aDyn) Vps1 and Drp1 exhibits unstructured loops i.e., B-insert and variable domain (VD) respectively, for protein-lipid interactions (Figure 1.4). Remarkably, classical dynamins have evolved a specialised pleckstrin-homology domain, necessary for membrane engagement.



Figure 1.4 Comparison of domain architecture in endocytic versus ancestral dynamins.

Colour codes depict similar structural elements and transparent boxes depict unstructured elements. Schemes depict N to C terminus from left to right. The blocks are not drawn to scale, indicated relative protein size is appropriate. Abbreviations as described in the text.

Experimental studies conducted *in vitro* with purified dynamin reveal that the dynamin trunk has a tendency to self-associate, resulting in the formation of tetramers in solution and helical frameworks on membrane surfaces^{82,77}. The dynamin helical polymer functions as a scaffold by inducing curvature upon the underlying membrane. When comparing the dynamin structure in its solution state and within the scaffold, substantial conformational alterations are evident. In aqueous environment, the foot remains tucked in due to its binding with the trunk; however, it becomes exposed upon interaction with the membrane. This exposure reveals additional sites for oligomerization on the trunk, which subsequently boosts the self-assembly of dynamin into a helical polymer⁸³. The scaffold formed by this helical polymer demonstrates several folds higher GTP hydrolysis activity also called ‘stimulated GTPase activity’ due to interactions between neighbouring head units^{84–86,36}. The resulting structural changes in the head cause the neck to bend, facilitating a closer alignment of the head and trunk. This is transmitted as a mechanical force through the neck to the trunk, leading to the foot digging deeper into the membrane causing progressive constriction of the underlying membrane and gradually destabilising it. This process generates a twisting force within the scaffold, ultimately culminating in severing of the underlying membrane beyond a critical point, simply referred to as membrane fission^{86,87}. In fact, purified dynamin has been shown to be sufficient to drive membrane fission⁷⁷.

Analysis of the super-constricted scaffold, achieved through a dynamin mutant with slow GTP hydrolysis, unveils that although interactions between inter-rung heads remain unchanged, the neck undergoes further bending^{83,88}. As a consequence, the trunk is compelled to push the foot more deeply into the membrane. Persistent interactions within the trunk permit the scaffold to adapt to varying curvatures, while slight rotations at these interfaces

accommodate significant alterations in the scaffold width and helical pitch. Intriguingly, mutations that lock the bending signalling element (BSE) in a bent configuration led to the halting of the fission process at a hemi-fission intermediate^{83,88}. Notably, mutations preventing bending impede the process of endocytosis. Recent findings from detailed simulations of dynamin monomers at both atomistic and coarse-grained levels underscore the structural significance of the BSE⁸⁹. Collectively, these findings establish a structural foundation for understanding how the scaffold generates mechanical stresses, ultimately leading to the constriction of the underlying tube.

1.6 Membrane-interacting ‘variable loops’ in the PH-domain

Although this domain is exclusive to endocytic dynamins setting them apart from their bacterial and mitochondrial counterparts, the PHD, characterized by a typical fold, is a recurring feature in numerous proteins with diverse functions, imparting them lipid-binding abilities⁹⁰⁻⁹². Structurally, the PHD fold comprises two antiparallel β -sheets and a C-terminal α -helix⁹³. The consecutive β -strands are connected by unstructured loops. The β -sheets and the α -helix remain highly conserved, and their collective fold determines the overall PHD structure. However, the loops exhibit a high degree of sequence variability among various proteins and are therefore referred to as "variable loops" (VLs), akin to the variable regions in antibodies that dictate antigen binding specificity. Interestingly, variable loops are conserved among endocytic dynamins suggesting a key role in dynamin function (Figure 4.1)^{52,94}. Specifically, the dynamin PHD stereo-specifically interacts with PIP₂, a phosphoinositide abundantly found on the inner leaflet of the plasma membrane^{95-97,91,98-100}. Early studies that reported the dynamin-PHD structure, annotate three variable loops (VLs), *viz.* VL1-3⁹³. The PH-domain in fact bears a polarised charge distribution¹⁰¹. The interface with the C-terminal α -helix is more acidic relative to the variable loop interface (Figure 1.5, Figure 1.7). The variable loops (VLs) are enriched with non-polar and basic amino acid residues that establish contact with the membrane through hydrophobic and electrostatic interactions. In dynamin1, the VL1 (531IGIMKGG) constitutes a loop with hydrophobic character, that is capable of inserting into the core of the membrane, and mutations that diminish its hydrophobic characteristics impede dynamin function resulting in defective membrane binding and fission^{102,103}. VL2 (554KDDEEKE) and VL3 (590NTEQRNVYKDY), relatively polar in nature, play pivotal roles in its functions. However, they do not directly insert into the membrane core; instead, they remain in close proximity to the membrane surface, exhibiting limited interactions

with negatively charged lipids¹⁰³. Specific VL-membrane interactions play a crucial role in dynamins' ability to bind to the membrane and carry out the fission process. Consequently, point mutations disrupting these interactions in VL1 (I533A), VL2 (E560K), or VL3 (Y600L) result in the impairment of clathrin-mediated endocytosis^{70,101,102,104,105}.

Biochemical studies have uncovered that while the affinity of a single PH-domain for PIP₂ is quite poor (in the millimolar range), the avidity of the PHD-PIP₂ interaction in the dynamin polymer falls in hundreds of nanomolar range^{96,99}. Reports also indicate that dynamin polymerisation sequesters or clusters PIP₂ molecules underneath the scaffold which facilitates membrane fission¹⁰⁸. This aligns with the notion that stable membrane anchorage by dynamin PHD releases dynamin auto-inhibition, which promotes self-assembly on the membrane and in-turn promotes more PHD-PIP₂ interaction while emphasizing that membrane binding and self-assembly are intricately coupled.

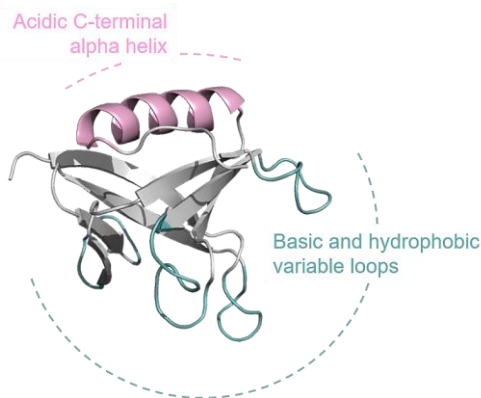


Figure 1.5 Structure of the dynamin pleckstrin-homology domain.

Dynamin PH-domain structure in solution highlighting the polarised interfaces of the domain. The beta sheets are anti-parallel (grey), the C-terminal alpha helix is enriched in acidic residues (magenta) and the variable loops connecting beta strands are enriched in basic or hydrophobic residues (cyan). The structure (PDB: 1DYN)⁹³ was self-annotated using ChimeraX^{106,107}.

1.7 The effector role of pleckstrin-homology domain in dynamin function

As among fission dynamins, only classical dynamins (cDyn) have evolved a specialized membrane-binding domain in comparison to the ancestral dynamins (aDyn); previous studies investigating the role of PH-domain in dynamin function have attempted to address whether the PH-domain confers any advantage in the modern design of the membrane fission catalyst. To this end, cellular studies have shown that expression of point mutants of membrane interacting residues in the PHD or Dyn^{ΔPHD} impedes internalization of cargo through CME¹⁰⁹.

It's noteworthy that mutations within the dynamin PH-domain which result in deficits in membrane binding *in vitro* and loss of function *in vivo*, do not appear to affect the protein's localization in cells^{108,101}. Studies have ascertained that dynamin's recruitment to the neck of nascent endocytic buds occurs via multimeric protein interactions¹¹⁰. This suggests that the PH-domain's role is not merely confined to targeting the protein, rather it has an active or effector role in dynamin function subsequent to dynamin recruitment at the site of action.

Furthermore, previous work from our lab where an engineered dynamin variant with the pleckstrin-homology domain (PHD) substituted for a 6xHis tag was examined in the context of membrane nanotubes containing chelator lipids, showed that the Dyn1 Δ PHD^{6xH} resulted in fission of supported membrane nanotubes¹¹¹. However, this fission reaction unfolded very gradually and the tubes exhibited a much-prolonged state of super-constriction. This indicated for the first time that the PHD contributes catalytically to dynamin function, in addition to providing a membrane binding interface. This, in fact, is consistent with the cellular functions of dynamins as the observed rates of mitochondrial fission by aDyn are staggeringly higher than the rate at which cDyn manages the release of clathrin-coated endocytic vesicles especially during synaptic vesicle recycling¹¹².

Much of our understanding of PHD-membrane cross-talk emerges from cryo-EM reconstruction of the membrane-bound dynamin polymer wherein the G-domains extend distally and PHD protrudes to rest atop the membrane, as opposed to being buried behind the stalk in solution⁸³. Dynamin stays auto-inhibited in solution as the PHD engages with the stalk blocking oligomerization interfaces, however, it is positioned such that the VLs extend outward and away from the stalk region. This orientation suggests the improbable likelihood of the VLs participating in maintaining dynamin in an autoinhibited state while in solution⁵². Once in proximity, the dynamin-PHD engages with the membrane and reportedly samples varied orientations on the membrane in the polymer¹⁰¹. This somewhat flexible interaction oversees the dynamics of dynamin polymerisation, signifying that PHD is a kinetic regulator of dynamin-mediated membrane fission. However, this aspect of PH-domain function is not exhaustively studied and requires further investigation.

1.8 Dynamin-PHD as a hub of congenital neuropathy & myopathy linked mutations

Notably, the pleckstrin-homology domain (PHD) has emerged as a hotspot for a whole host of mutations associated with congenital disorders classified under the umbrella of

centronuclear myopathy (CNM) and Charcot-Marie-Tooth (CMT) neuropathy (Figure 1.6). Mutations linked to CMT are concentrated within regions of the PHD associated with membrane binding, while CNM-linked mutations are located in other segments of dynamin PHD^{113–120}. It is therefore essential to examine PHD-membrane interplay at the molecular level to comprehend the fundamental role of PH-domain in dynamin function towards achieving a detailed molecular picture of defects that arise during physiological disorders linked to perturbed dynamin PH-domain function, thereby aiding therapeutics.

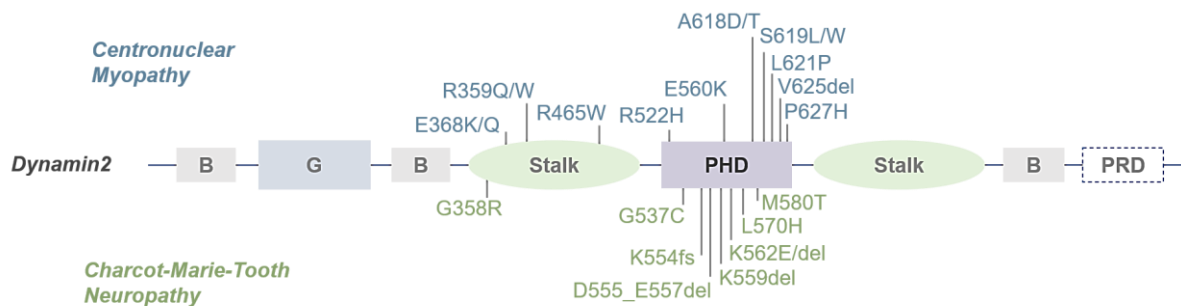


Figure 1.6 Dynamin domain architecture highlighting disease-linked mutations.

As is apparent from the figure, the dynamin PH-domain is a hotspot of pathological mutations associated with centronuclear myopathy (top, blue) and Charcot-Marie-Tooth neuropathy (bottom, green). Illustration self-curated by adaptation of published data¹²¹.

It is apparent that in cells, a number of precise and dynamic interactions orchestrate the PHD-membrane engagement to manifest efficient membrane-fission and vesicle release by dynamin, downstream of its SH3-PRD mediated recruitment to CCPs^{30,110}. In this scenario, as membrane binding mutants of dynamin localise to CCPs, it remains difficult to ascertain their effect from the complex cellular environment. Substantiating these models biochemically has also remained challenging, primarily due to the fact that reconstitution assays particularly rely on lipid-based membrane recruitment of purified dynamin wherein membrane-binding mutants do not even recruit to the so called ‘site of action’, in this case the lipid nanotube. The dynamic nature of PHD-membrane cross-talk presents as a restraint in obtaining high-resolution structures^{101,103}. Even in cryo-EM studies where the reported resolution of the dynamin polymer close to ~ 3.4 Å on membrane was achieved, the PHD remained rather poorly resolved i.e., ~ 7 Å making it difficult to map out residue level interactions that could shed light on the molecular interactions in physiology and disease⁸³.

1.9 Key findings from molecular dynamics simulations and structural modeling

To discern the molecular details underlining the kinetic role of PHD in dynamin function, *in-silico* analysis presents as a resource. Intriguingly, a yet unannotated novel variable loop i.e., VL4 between residues 576 and 583 becomes readily apparent in the dynamin PHD structure, flanked by the $\beta 5$ and $\beta 6$ strands (Figure 1.7)^{103,94,52}.

Recent atomistic molecular dynamics (MD) simulations of the isolated dynamin PHD with the membrane reaffirm membrane insertion of VL1 where the IsoLeu533 residue dips about 0.45-0.55nm below the phosphate plane, consistent with previous literature¹⁰³. Further, MD simulations unveil that the novel VL4 also inserts into the membrane, and the PHD exhibits the capability to explore multiple orientations on the membrane by utilizing VL1 and VL4 as flexible pivot points. This observation is rather surprising, particularly considering that VL4 (576EKGFMSSK) possesses substantially lower hydrophobicity compared to VL1 (531IGIMKGG). Surprisingly, simulations with the VL4 tip mutant *PheAla579Ala* or *F579A* showed no apparent defect in membrane binding. Instead, this mutant showed an enhanced conformational flexibility of the PHD on the membrane¹⁰³.

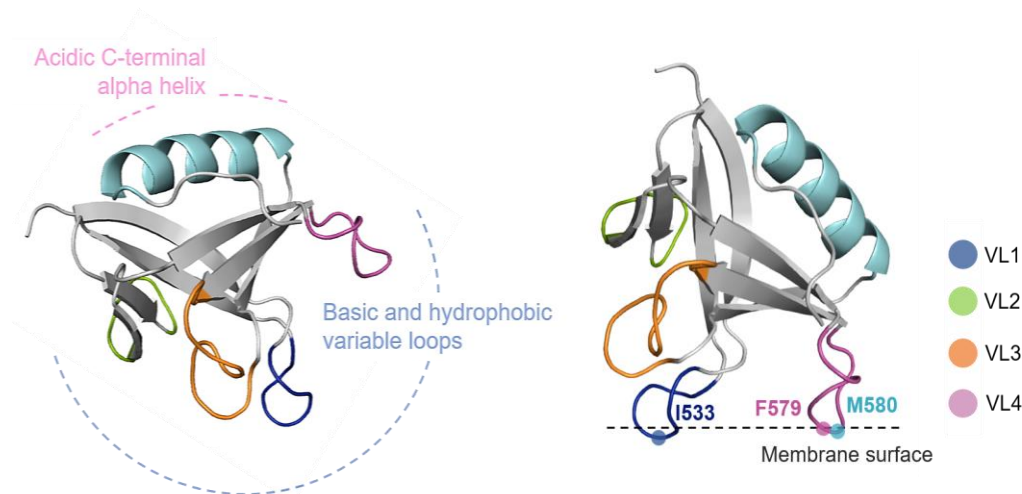


Figure 1.7 Variable loops in the dynamin pleckstrin-homology domain.

Dynamin PH-domain structure in solution (left) highlighting the polarised interfaces of the domain. Depiction of orientation of dynamin PHD on the membrane (right) to highlight variable loops and relevant residues that are seen to dip into the membrane in MD simulations. Dynamin PHD structures (PDB: 1DYN)⁹³ were self-annotated using ChimeraX^{106,107}.

Of particular significance, the structural modeling of dynamin monomers within the cryo-EM map of the scaffold corroborates the notion of VL1 and VL4 being the primary anchors to the membrane^{94,52}. Additionally, the modeling data reveals that certain PHDs within the polymer also exhibit the insertion of VL2 and VL3 into the membrane. Importantly, a missense mutation *Met580Thr* at the tip of VL4 (Figure 1.7), adjacent to the membrane dipping residue PheAla579 revealed by MD simulations, has been linked to an autosomal dominant form of CMT¹¹⁶. Together, these results form the basis of this study, aimed at testing the contribution of the novel membrane anchor VL4 in PHD-membrane engagement and in-turn its significance on dynamin-mediated membrane fission.

Chapter 2

MATERIALS AND METHODS

2.0 Materials and Methods

All materials used through the course of this work along with detailed methodology are described in appropriate sections below. For commercially sourced items, the corresponding vendors and catalog numbers are indicated in brackets. Figures in this section are self-curated. Contributions or citations have been duly indicated wherever applicable.

2.1 Constructs, cloning, and plasmids

Constructs and cloning: For bacterial expression, the human dynamin1 gene and BIN1 (bridging-integrator-1 or box-dependent Myc-interacting protein-1) gene (human, isoform 8, amplified from addgene plasmid #27305) were cloned separately into a pET15b vector with an amino-terminal (N-terminal) hexa-Histidine (6xHis) and a carboxy-terminal (C-terminal) StrepII tag downstream of a T7 promoter, containing an ampicillin selection marker. Human dynamin 2 gene was cloned in a pET15b vector with a C-terminal StrepII tag only downstream of a T7 promoter, containing an ampicillin selection marker. For mammalian cell expression, human dynamin1 was amplified out of the pET15b plasmids and cloned into a pcDNA3.0 vector with a C-terminal GFP fusion, downstream of a CMV promoter.

Note: PCR-based Restriction-free (RF) cloning was used to clone all genes into desired vectors as well as to introduce mutations in dynamin plasmids.

Plasmid-prep: Plasmids were amplified in and isolated from *E. coli* DH5 α cells using the alkaline lysis method. The plasmids were finally purified using Miniprep columns (Qiagen, 27106) and stored at -80 °C for future use. All clones were confirmed by sequencing.

2.2 Protein expression, purification and fluorescent labelling

Protein-expression: Dynamin and BIN1 clones were transformed in BL21(DE3) cells and plated under Ampicillin selection. Several colonies from this plate were inoculated in a 10 ml LB broth medium with ampicillin and grown for 4-6 hours at 37 °C in a shaker incubator. This primary culture was inoculated (1% inoculum) and grown in 1L autoinduction medium under ampicillin selection at 18 °C for 36 hours. Bacterial cells were pelleted from 1L culture each, rinsed with 1x PBS (phosphate buffer saline) and stored at -40 °C for further use.

Protein-purification: The frozen bacterial pellet was thawed in 30 ml of lysis buffer containing 20 mM HEPES pH 7.4 and 500 mM NaCl (HBS₅₀₀) with 1x PIC (protease inhibitor

cocktail, Roche 5892791001) and 1x PMSF or phenylmethylsulfonyl fluoride, (Sigma P7626), then lysed by intermittent sonication in an ice-water bath until the solution was homogenous. Lysate was then spun at 30,000 g in a fixed angle rotor at 4 °C for 20 minutes in oak ridge tubes (Nalgene centrifuge tubes, Oak Ridge Style 3119) and supernatant was separated from the pellet fraction for further processing. For proteins containing the 6xHis and StrepII tags (dynamin1, BIN1 and BIN1-GFP), the supernatant was incubated with HisPur™ Cobalt Resin (Thermo Fisher Scientific, 89965). The resin was first washed with Millipore water to remove ethanol from the slurry, and then equilibrated with HBS₅₀₀. The supernatant was bound to the pre-equilibrated beads under rocking at 4 °C and then loaded on to a PD10 column. The unbound proteins were washed off using the equilibration buffer HBS₅₀₀ and the bound protein was eluted with 100 mM EDTA in HBS₅₀₀. The elution was loaded onto a StrepTrap HP column (GE Lifesciences, 28-9075-46), pre-equilibrated with HBS₅₀₀, washed with buffer containing 20 mM HEPES pH 7.4 and 150 mM NaCl (HBS₁₅₀). Finally, the bound protein was eluted with 2.5 mM desthiobiotin (Sigma, D1411) in HBS₁₅₀.

Note: Dynamin1 full-length co-elutes with a partial C-terminal truncation product despite the meticulous two-step purification with dual affinity tags on either terminus to ensure full-length product purification, likely because it exists predominantly as a tetramer in solution and monomeric species lacking the tags could be eluted by virtue of them being a part of the tetrameric species. This species only becomes apparent on an SDS-PAGE gel due to the denaturing conditions.

For dynamin2, the supernatant separated from the lysate after the 30,000 g spin was loaded directly onto a StrepTrap HP column pre-equilibrated with HBS₅₀₀, and then washed with 100 mM EDTA in HBS₅₀₀ to ensure removal of any bound nucleotides in this one-step purification process. Thereafter, unbound proteins were washed off with excess HBS₅₀₀ which was then exchanged for HBS₁₅₀. The bound protein was eluted with 2.5 mM desthiobiotin in HBS₁₅₀. Strep II tag affinity purifications were done using fast performance liquid chromatography (AKTA Prime Plus FPLC system, 11-0013-13)

Protein-prep: All purified proteins were stored on ice in 4 °C for the duration of the experiments or stored frozen with 10% glycerol at -80 °C for longer term use. Glycerol was removed with extensive dialysis in dialysis bags (Thermo Scientific Snakeskin dialysis tubing, 68100) after thawing the proteins. All proteins were spun at 100,000 g to remove aggregates before use in any assay. For estimating protein concentration, freshly spun protein was aliquoted in Quartz cuvettes, absorbance spectra were scanned using UV spectrophotometer

(Shimadzu UV-1800) and absorbance peak at 280 nm was noted after correcting for background with the appropriate buffer. The protein concentration was then estimated using the correlation from beer-lambert law i.e. $A = \epsilon cl$, where A is the absorbance, ϵ is the molar extinction coefficient, l is the path length in cm and c is the concentration. The respective molar extinction coefficients (ϵ) of the proteins were predicted by inputting full protein sequences in the Expasy ProtParam tool.

Fluorescent labelling: Alexa488 C5-maleimide or Alexa594 C5-maleimide (Invitrogen, A10254 or A10256) stock solutions were prepared by arbitrarily dissolving a minute amount (on a tip) of the dye powder in 10 μ l DMSO. The concentration of this stock was estimated in methanol after appropriate serial dilution using the corresponding absorbance maxima peaks obtained on the UV spectrophotometer. For the labelling reaction, purified and freshly spun dynamin1 was incubated with fivefold molar excess of the respective dye in HBS₁₅₀ for one hour at RT in dark. The reaction was quenched with excess dithiothreitol (DTT), and the unreacted dye was removed by extensive dialysis against HBS₁₅₀ and stored on ice in 4 °C for the duration of the experiments. Labelled protein was also spun down and prepped before use in assays, as described above.

2.3 Liposome preparation

Lipid stocks: Chloroform stocks of 1,2-dioleoyl-sn-glycero-3-phosphocholine (DOPC) and 1,2-dioleoyl-sn-glycero-3-phospho-L-serine (sodium salt) (DOPS) were obtained from Avanti Polar Lipids and stored at -80 °C. 1,2-dioleoyl-sn-glycero-3-phospho-(1'-myo-inositol-4',5'-bisphosphate) (ammonium salt) i.e. PI(4,5)P₂ was obtained as a powder from Avanti Polar lipids and dissolved in Methanol, then stored at -80 °C in glass vials (Supelco, Sigma, 27134). The UV-activable probe i.e., diazirine-containing fluorescent lipid conjugated with BODIPY or BODIPY-diazirine phosphatidylethanolamine (BDPE) was prepared in the lab by using SDA-diazirine (Sigma, 803413) and 1-palmitoyl-2-dipyrrometheneboron difluoride-undecanoyl-sn-glycero-3-phosphoethanolamine (TopFluor PE, Sigma, 810282P) as described before^{122,123}.

Lipid aliquoting: A glass tube was thoroughly cleaned by washing with 1% sodium dodecyl sulphate (SDS) solution, then methanol and finally chloroform. The residual chloroform was dried off using a gentle stream of air through a filter using a blower. The lipids were aliquoted at desired ratios (as per mole fractions) in the clean glass tubes, then dried to obtain a thin film

of lipid using a gentle stream of air. The tube was left under high vacuum for at least 3 hours to allow complete solvent evaporation and proper drying.

Lipid hydration: Warm (50 °C) deionized water was added to the glass tube containing dried lipids, to achieve a final concentration of total 1 mM of lipid. The glass tube was properly covered and left in a water bath at 50 °C for 30 min to allow gentle hydration of lipids followed by subsequent swelling and formation of liposomes. The tube was eventually vortexed vigorously to ensure all the dry lipid was recovered in-solution and then extruded using an assembly of extrusion apparatus (pre-cleaned) through 100 nm pore-size polycarbonate filters (Whatman, 800309).

2.4 GTPase activity assays

Purified dynamin1 (0.1 μM) was incubated with 1 mM GTP (Jena Bioscience, NU 1012) and 1 mM MgCl₂ with or without 100 mole percent DOPS containing liposomes (10 μM) in HKS₁₅₀ (20 mM HEPES pH 7.4, 150 mM KCl) at 37 °C. A particular aliquot of this reaction was taken from the reaction mix and added to a microplate well containing 0.5M EDTA to quench the reaction, at different time points ranging between 0 to 30 minutes. Malachite-green based colorimetric assay was used to estimate the released inorganic phosphate¹²⁴. The absorbance of each well was noted at 630 nm using a micro plate reader (Tecan, Infinite M200 Pro). To arrive at concentrations of the released inorganic phosphate upon GTP hydrolysis by dynamin, a 250 μM stock solution of dibasic sodium phosphate (Na₂HPO₄) was used to obtain a standard curve between 0 to 200 μM phosphate and the unknown values were derived by interpolation.

2.5 Liposome co-sedimentation assay

Purified dynamin1 (1 μM) was incubated with 100 mole percent DOPS containing liposomes (100 μM) at room temperature undisturbed for 30 minutes. As a control, equivalent dynamin1 was left at in a tube at room temperature without liposomes undisturbed for 30 minutes. The reactions were then spun at 100,000 g at 25 °C for 30 minutes in a tabletop ultracentrifuge (Beckman Coulter, Optima Max-XP, 393315). The liposomes bound with protein due to being denser sediment, whereas unbound liposomes or proteins stay afloat. The supernatant and pellet fractions are then separated carefully and analysed using SDS-PAGE after normalising volumes in both the fractions. Figure 2.1 shows a workflow schematic.

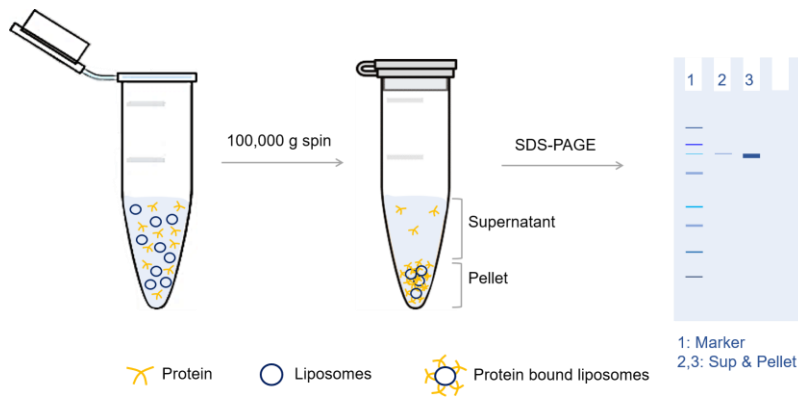


Figure 2.1 Schematic depicting the workflow of a liposome co-sedimentation assay.

Protein is spun at 100,000 g prior to the assay to remove any aggregates or higher-order oligomers. The resultant protein concentration is estimated and then used in the assay as shown. The pellet and supernatant fractions are separated and analysed using SDS-PAGE.

2.6 Proximity-based labelling of membrane-associated proteins (PLiMAP)

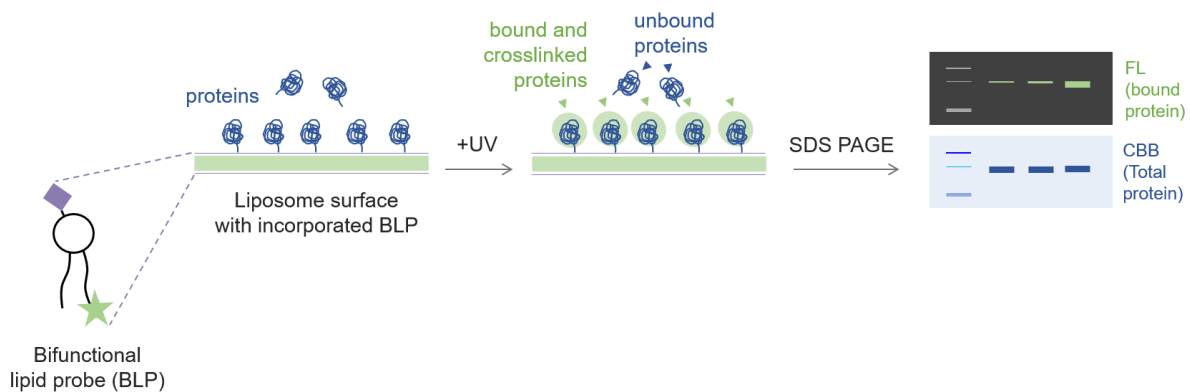


Figure 2.2 Schematic depicting the workflow of a PLiMAP assay.

Proximity-based labelling of membrane-bound proteins works on the principle that a reactive headgroup probe (purple) promiscuously reacts with other molecular species which are in its close proximity upon acute UV activation. This reaction results in covalent crosslinking of reactive species (here, lipids and proteins). The proteins are resolved using SDS-PAGE. Since the crosslinked lipid moiety also has a fluorescent probe attached to its tail (green star), the bound and crosslinked proteins acquire fluorescence signal. A gel image captured under fluorescence channel (FL) represents relative binding across reactions and an image captured after Coomassie brilliant blue staining (CBB) represents total proteins in each reaction.

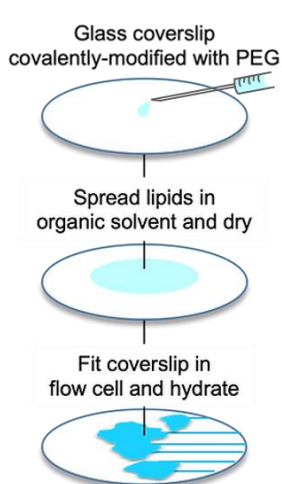
For analysis of dynamin binding on highly anionic membranes, liposomes containing 99 mole percent DOPS and 1 mole percent BDPE were mixed with purified dynamin1 at a 100:1

lipid to protein molar ratio in a final volume of 30 μL in HBS_{150} . These reactions were incubated in the dark at room temperature for 30 minutes and then exposed to a pulse of 365 nm UV light (UVP crosslinker CL-1000L) at an intensity of 200 mJ cm^{-2} for 1 minute. The reaction was mixed with sample buffer, boiled, and resolved using SDS-PAGE. As a control, corresponding reactions without UV exposure were also processed similarly. Gels were first imaged for BODIPY fluorescence on an iBright1500 (Thermo Fischer Scientific) and later fixed and stained with Coomassie Brilliant Blue (CB). Binding data were fitted to a one-site binding isotherm using GraphPad Prism. Methods performed as previously described^{122,123}.

For analysis of dynamin binding on membranes mimicking physiologically relevant lipid composition, dynamin1 was mixed with liposomes containing 83 mole percent DOPC, 15 mole percent DOPS, 1 mole percent PI(4,5)P₂ and 1 mole percent BDPE at a 100:1 lipid to protein molar ratio in a final volume of 30 μL in HBS_{150} , exposed to a short UV-pulse as described above and then analysed after SDS-PAGE to arrive at one-site binding isotherms.

2.7 Supported Membrane Template (SMrT) preparation, assays and analysis

Template preparation: Supported membrane templates (SMrT) were prepared in a flow-cell as described earlier^{80,125}. To make the templates, lipids were aliquoted at desired ratios to a final concentration of 1 mM in chloroform in a glass vial (Supelco, Sigma, 27134) along with a fluorescent lipid DHPE-TexasRed (Invitrogen, T1395MP) doped at 1 mole percent concentration in the said mix. 1-2 μL of the lipid mix was spread with a glass syringe



(Hamilton, 80000) on a PEGylated glass coverslip (prepared as previously described^{80,125}), dried, and assembled inside an FCS2 flow chamber (Biopetechs, 060319-2). The chamber was filled with HBS_{150} and flowed at high rates to form supported membrane templates. The region where the lipid is initially spread forms a planar supported lipid bilayer or SLB post-hydration. Due to sheer flow of buffer through the chamber, this bilayer reservoir gets extruded into an array of tubes of varied diameters, partially tunable with flow rates and spacer dimensions that lay pinned on the glass surface across their length.

Figure 2.3 Schematic depicting supported membrane templates' preparation workflow. Image modified from /pucadyillab.com, original by Thomas Pucadyil.

Membrane-binding analysis: Templates were prepared by spotting 1 μ l of a 1 mM lipid mix containing 83 mole percent DOPC, 15 mole percent DOPS, 1 mole percent PI(4,5)P₂ and 1 mole percent DHPE-TexasRed in HBS₁₅₀. Images of the SLB and tubes were captured to record the before dynamin state, then 0.3 μ M dynamin conjugated with Alexa488 C5-maleimide was flowed onto the templates in HBS₁₅₀ and incubated for 10 minutes. Excess dynamin was washed off with HBS₁₅₀ and templates were then imaged. Number of tubes displaying scaffolds of bound dynamin were counted. Tubes with at least one corresponding dynamin puncta were counted and plotted against total number of tubes samples, to report binding probability of dynamin within an experiment for both the WT protein and mutants.

Membrane-fission analysis: Templates were prepared similarly as described in the binding analysis above and then pre-equilibrated with an oxygen scavenger cocktail in HBS₁₅₀. Time-lapse images were acquired while flowing in 0.3 μ M dynamin mixed with 1 mM GTP (Jena Bioscience, NU 1012) and 1 mM MgCl₂ in HBS₁₅₀. The fission probability was determined by counting the fraction of tubes displaying at least one cut.

Note: For both binding and fission assays involving BIN1, 0.2 μ M of BIN1-GFP or BIN1 was flowed onto the templates and incubated for 10 minutes. Unbound protein was washed off with HBS₁₅₀ before flowing in dynamin with or without GTP and 1 mM MgCl₂ in HBS₁₅₀.

Fluorescence-based tube radius analysis: To determine tube sizes, a calibration procedure, previously detailed^{125,80}, was employed. This is discussed in detail in section 6.1.

2.8 Cell culture and transferrin uptake assay

Cell Culture: Dynamin2 KO HeLa cells were a generous gift from Mike Ryan's lab at Monash University, Australia. These cells have been reported before³⁹. The cells were cultured in complete DMEM (HiMedia, AL007A) with 10% foetal bovine serum or FBS (HiMedia, RM10432) and 1% penicillin-streptomycin (HiMedia, A001) and maintained in a humidified 5% CO₂ incubator at 37°C.

Transient transfection: Cells were seeded in 60 mm culture dishes on 40 mm glass coverslips (Bioprotech). At ~70% confluency, cells were incubated in OptiMEM with 1 μ g of the dynamin plasmid using Lipofectamine 2000 (Thermo Fisher Scientific). OptiMEM was replaced for complete DMEM 4-6 hours post transfection.

Transferrin uptake assay: Transferrin uptake experiments were performed 24 to 48 hours post-transfection. Prior to transferrin feeding, cells were serum-starved for 2 hours in serum-free DMEM. Subsequently, the cells were washed twice with HEPES-buffered Hank's balanced salt solution (HBSS) and then the coverslip was assembled in an FCS2 chamber maintained at 37 °C. The cells were fed 50 $\mu\text{g mL}^{-1}$ TexasRed labelled transferrin (Invitrogen, T-2875) and incubated for 10 minutes in HBSS. Unbound transferrin was washed off before imaging the cells in HBSS at 37 °C.

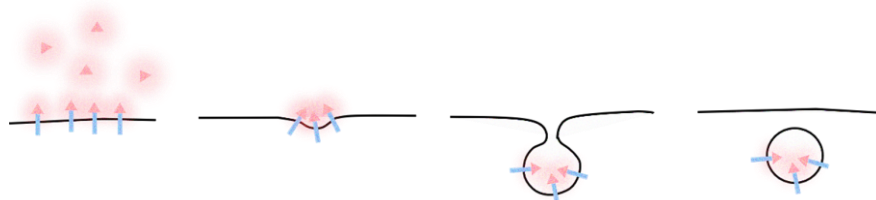


Figure 2.4 Schematic depicting a transferrin uptake assay.

Black line represents the plasma membrane, where endocytosis takes place. When fluorescently tagged transferrin ligand (glowy red arrow heads) is added to cells, it readily binds the transferrin receptor (blue arrows) displayed on the cell surface and is internalised through CME which depends on dynamin catalysed membrane fission. Excess ligand is washed from the chamber and then only internalised transferrin fluorescence remains apparent as punctae in the cell. An estimate of total internalised transferrin fluorescence is therefore a measure of efficiency of endocytosis and in-turn dynamin functions.

2.9 Fluorescence imaging and image analysis

Imaging of SMrT templates and cells was done using a 100 \times , 1.4 NA oil-immersion objective lens and cell-imaging was done using a 60 \times , 1.4 NA oil-immersion objective both on an Olympus IX83 inverted epifluorescence microscope. This microscope was equipped with both an LED light source (CoolLED) and an Evolve 512 EMCCD camera from Photometrics for image capture. The process of image acquisition was run and managed by the software MicroManager, while subsequent image analysis was performed using Fiji¹²⁶.

Quantification of transferrin uptake was done by measuring the minima and maxima of Tx-Red transferrin fluorescence intensities within marked regions defining cell boundaries. Background correction was achieved by subtracting the minima from maxima with additional correction for autofluorescence in cells, obtained from cell images captured before adding transferrin. To account for variations in Tx-Red transferrin fluorescence intensities across experiments, the background-corrected intensities in transfected cells were normalized to the mean intensity observed in non-transfected cells for each individual experiment.

Chapter 3

BRIEF RATIONALE:

A PRELUDE TO THE RESULTS

3.0 Brief rationale: A prelude to the results

Ample literature sheds light on the fact that the *pleckstrin homology domain* or PHD has an effector role in dynamin-mediated membrane fission, beyond targeting the molecule to the growing vesicle^{101,108} as is discussed in *Chapter 1*. Biochemical studies have identified that the PHD has a catalytic contribution in dynamin-mediated membrane fission¹¹¹. However, a molecular understanding of this function is lacking at present.

Molecular dynamics (MD) simulations aimed at understanding PHD-membrane dynamics, uncover the presence of a novel membrane-inserting loop, variable loop 4, that seems to stabilize the dynamin PH-domain on the membrane in addition to the previously known VL1¹⁰³. The highly conserved nature of variable loops among dynamin homologs suggests their importance for dynamin function^{94,52}. Additionally, loop insertion into the membrane has been known to modulate the physical properties of the underlying membrane^{103,127}. Here, VL1 and VL4 membrane-insertion decreases the bending modulus of the underlying bilayer, making it more amenable to fission. Together these could potentially serve as membrane anchors securing dynamin-PHD onto the membrane.

Interestingly, simulations of the F579A mutant within the isolated PHD context did not reveal any apparent defects in membrane binding. However, this apparent discrepancy can be attributed to the fact that membrane dissociation would be favoured in the full-length protein compared to an isolated PHD simply due to the allowed orientations of degrees of freedom. Consequently, even a subtle reduction in the hydrophobicity of VL4 could have a more significant impact on membrane partitioning properties in the context of the full-length protein than in the isolated PHD. Moreover, the simulations are performed with isolated dynamin PHDs on planar membrane patches, instead of a curved membrane tube that might display more membrane defects presenting more binding sites for variable loops extending in a scaffolded dynamin polymer. Each of these aspects could lead to contrasting results but remain entirely unexplored.

Structural modeling in the cryo-EM map of dynamin polymer on a membrane tube confirms VL1 and VL4 as preferred membrane anchors. However, there has been no experimental proof supporting significance of the novel VL4 in dynamin function. In fact, VL4 mutations when tested in simulations do not show any apparent effect unlike VL1 mutants, which significantly affect PHD-membrane binding^{94,52}.

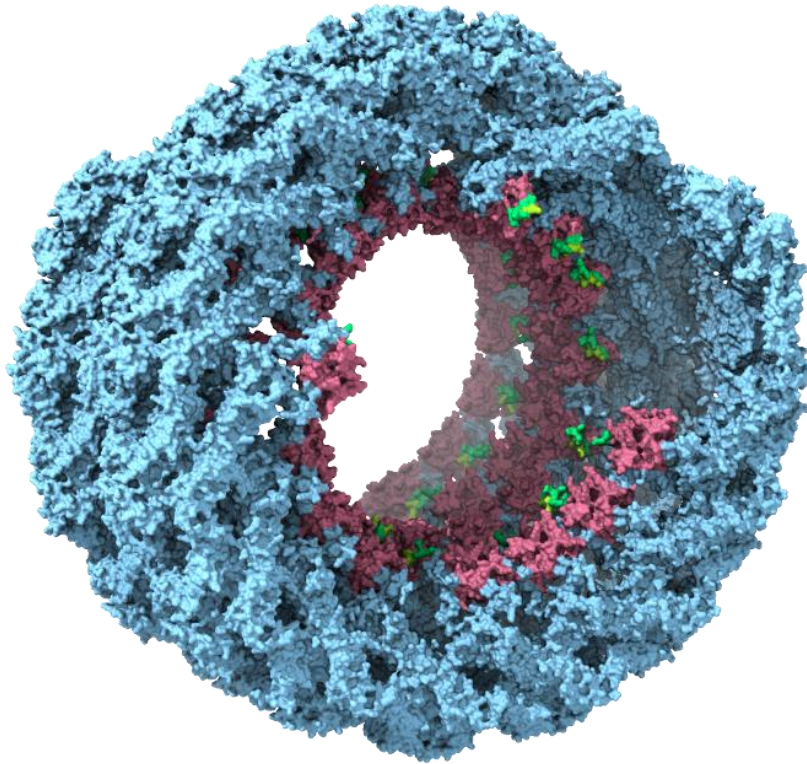


Figure 3.1 Surface rendered structural model of a dynamin polymer.

The doughnut shaped structure represents 23 dynamin dimer subunits or 46 monomers individually modelled into the cryo-EM structure of dynamin polymer assembled on anionic membranes previously reported⁸³. The head, neck and trunk are annotated in cyan; the foot is in magenta, yellow highlights PheAla579 and Met580 at the tip of green VL4. Figure reproduced from reference⁵².

These remarkable yet contrasting findings about the novel VL4 and its association with disease pathology prompted us to probe the significance of VL4 in dynamin function. In order to mechanistically link data from MD simulations to the CMT neuropathy, we analysed the VL4 mutants F579A and M580T in a suite of in vitro assays analysing membrane binding, fission and monitored how expression of this mutant affects CME in cells. While the essential role of VL1 has been well established, the work discussed in this thesis is the first to investigate the significance of VL4 to dynamin functions.

Chapter 4

**PROBING DYNAMIN FUNCTIONS ON HIGHLY
ANIONIC MEMBRANES**

4.0 Probing dynamin functions on highly anionic membranes

Dynamin has been reported to efficiently bind and sever negatively charged membranes^{77,49,51}. In order to proceed with addressing VL4 functions in dynamin-mediated membrane fission, we first analysed dynamin functions on membranes with high anionic character. Here, we used membranes containing 100 mole percent of the negatively charged phospholipid phosphatidylserine (DOPS).

4.1 The *variable loops* in dynamin PHD are highly conserved regions

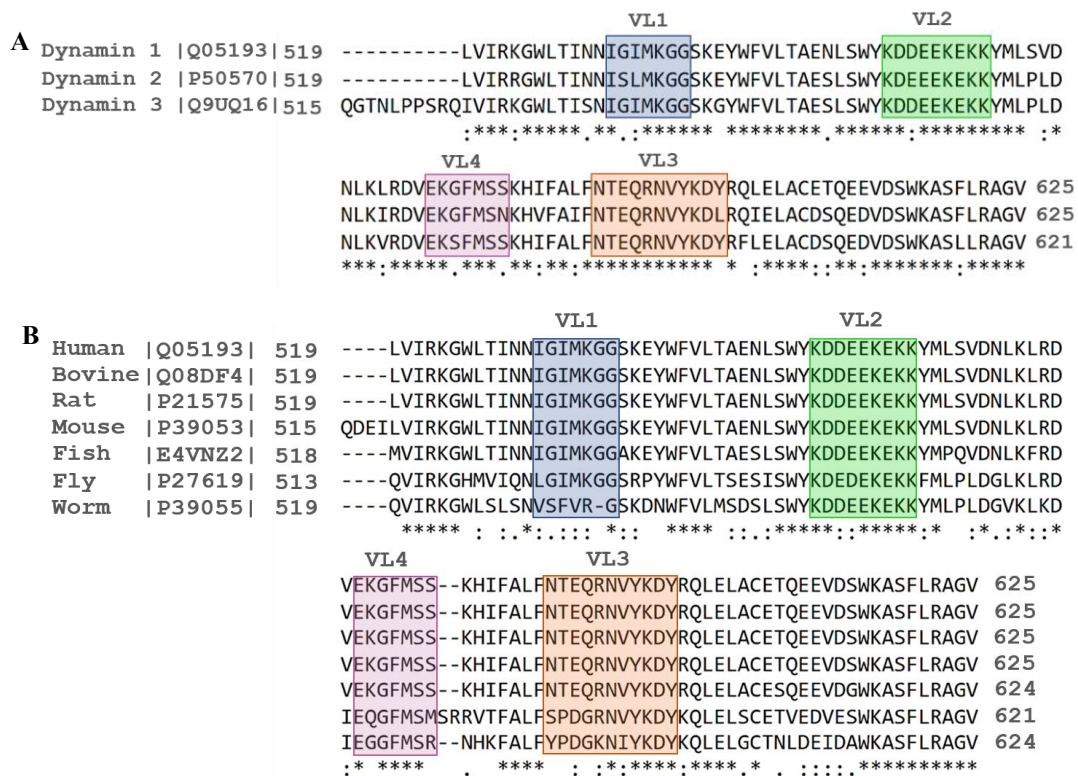


Figure 4.1 Sequence alignment of dynamin pleckstrin-homology domain.

A. Human dynamin paralogs. **B.** Dynamin homologs from various species across evolution. Variable loops are colour coded as shown. Each uniprot ID is indicated before the sequence.

The conservation of primary sequences in proteins across evolution is testament to their indispensable need for protein functioning. We know that endocytic dynamins show a high degree of conservation in the variable loops. As a primary exercise, we performed sequence alignment analysis on dynamin homologs from various eukaryotic species. Remarkably, the so called ‘variable loops’ demonstrate a stark degree of conservation across evolution (Figure 4.1). In fact, only a few conservative substitutions are seen among mammalian dynamin1/2/3

PH-domains, testament to the fact that the mechanism of dynamin function is likely overall conserved among its homologs. These stretches that make up the connecting threads between subsequent beta strands are likely to be highly relevant for dynamin functions. While the importance of VL1-3 has been described by earlier studies but is not explored for VL4.

To specifically understand VL4 relevance in dynamin function, we introduced a point mutation at the tip of VL4 *PheAla579Ala*. Phenyl alanine being a non-polar residue, comes closest to the underlying membrane as shown by AMD simulations¹⁰³. Purified dynamin is known to bind, tubulate and upon GTP-hydrolysis, sever negative charged membranes. We recombinantly purified dynamin 1 (F579A) and tested its functions on liposomes displaying high negative charge.

As dynamin1, dynamin1 F579A also purified with a C-terminal truncation despite two step purification with dual affinity tags at either terminus, and therefore migrated as a doublet when analysed using SDS-PAGE gel.

4.2 Testing a VL4 tip mutant with reduced hydrophobicity - Dynamin1 F579A

Dynamin1 F579A displays VL4 with slightly reduced hydrophobicity. This is a mutation more subtle as compared to the pathogenic CMT-linked mutation i.e., M580T in the adjacent residue that more dramatically alters VL4 hydrophobic character. In order to analyse VL4 functions, we first analyse the activity of the VL4 tip mutant Dynamin1 F579A (Figure 4.2).

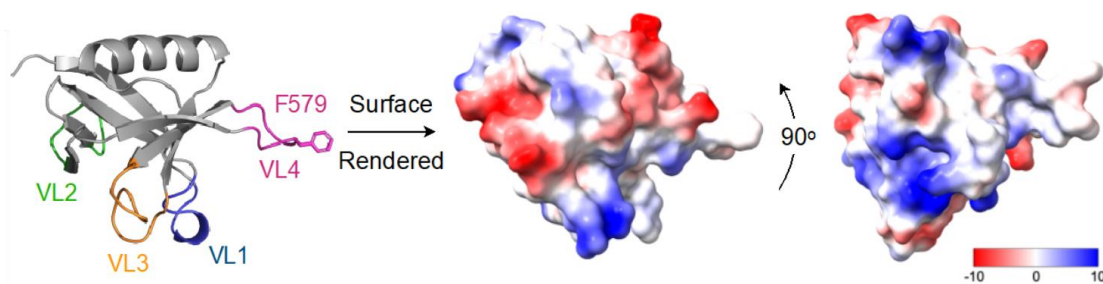


Figure 4.2 Surface rendered model of dynamin PHD highlighting charge distribution.

The dynamin1 PHD crystal structure (left, PDB: 1DYN)⁹³ is depicted here, highlighting the four variable loops labelled as VL1-4. Specifically, the F579 residue within VL4 is indicated. In the middle and right panels, the space-filling model of the structure are shown, illustrating the charged surfaces located on the side. The positively charged surfaces are responsible for binding to the membrane. The surface rendered model was generated using ChimeraX^{106,107}.

4.2.1 *GTP-hydrolysis activity*

The variable loops are unstructured loops lying in regions that face away from the stalk. Mutations in the variable loops are not likely to alter intra molecular interactions between the PHD and the stalk or affect overall folding of the protein. However, to first validate that the mutant protein dynamin1 F579A indeed folds properly and displays proper function, we tested its basal capacity for GTP-hydrolysis in solution. In addition, dynamin is known to display stimulated GTPase activity when assembled as a polymer on membranes by virtue of head-head interactions in subsequent rungs. We also tested stimulation in dynamin's GTPase activity on membrane containing 100 mol% DOPS. We found that dynamin1 F579A shows basal and stimulated GTPase activity comparable to that of dynamin1, indicating the protein is properly folded and active (Figure 4.3).

4.2.2 *Membrane binding*

Next, we tested dynamin1 F579A for membrane binding. To do this, we resorted to the widely-used liposome co-sedimentation assay to score for membrane binding. Dynamin1 WT and F579A were incubated with highly anionic liposomes (100 mole percent dioleoyl-phosphatidylserine or DOPS) and the subjected to high-speed centrifugation to separate the membrane-bound (pellet) and unbound (supernatant) fractions. Similar amounts of dynamin1 WT and F579A were seen to partition in the pellet indicating no gross defect in membrane binding by dynamin1 F579A. However, a fraction of dynamin1 partitioned in the pellet even control reactions set up without liposomes, due to dynamin's inherent capability to self-associate into higher-order oligomers which can pellet down at such high-speed spins (Figure 4.3). Therefore, it remained difficult to quantitatively assess the membrane-binding in this case.

To circumvent this anomaly, we utilized a novel sensitive assay^{122,123} developed in the lab to test membrane-binding of dynamin1 F579A to highly anionic liposomes. Here, the liposomes were made with 99 mole percent of DOPS and 1 mole percent of the bifunctional lipid probe that displays a cross-linkable moiety at the headgroup and a fluorescent reporter at its tail for proximity labelling of membrane associated proteins or PLiMAP. The primary advantage of such an assay is that it allows for preferential labelling of membrane-bound fraction of the protein, therefore excluding the soluble fraction without subjecting the reaction to high-speed centrifugation for separation.

Upon UV-exposure, membrane-associated or membrane-bound proteins get crosslinked to the lipid probe which carries a reactive moiety on its head and a fluorophore (here, BODIPY) on its tail, helpful in distinguishing bound from unbound protein. As a result, the fraction of protein bound to the membrane gets covalent attached to the lipid probe, which can easily be analysed using SDS-PAGE. The bound protein fraction lights up as fluorescent bands when imaged for the BODIPY signal, whereas total protein in the reaction remains equal across varying conditions which can be seen in coomassie brilliant blue stained gel. Control reactions were set up either using liposomes displaying DOPC (dioleoyl-phosphatidylcholine), the zwitterionic lipid instead of DOPS or by not exposing the reaction to UV therefore validating both, the method and specific binding of the protein to negatively charged membranes.

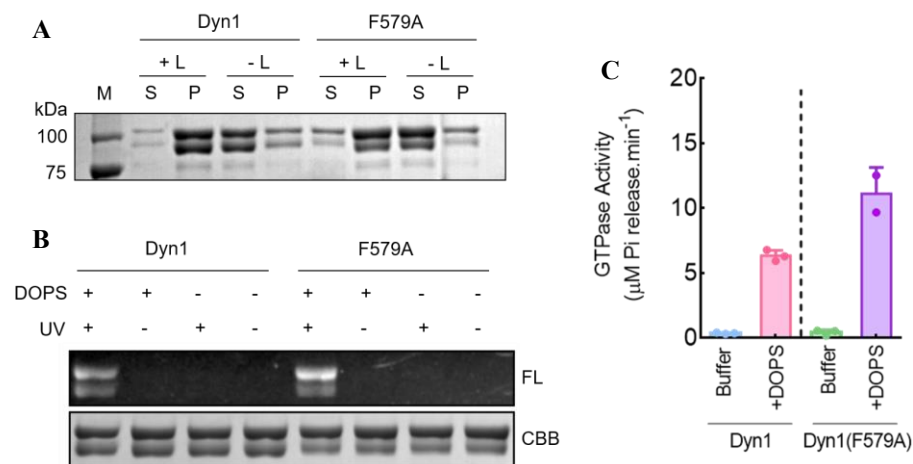


Figure 4.3 Dyn1 membrane binding and GTP hydrolysis on highly anionic membranes.

Representative gel showing **A**. liposome co-sedimentation assay and **B**. in-gel fluorescence (FL) and Coomassie brilliant blue (CB) staining of Dyn1 and the VL4 mutant on liposomes containing 100 mole percent DOPS. Appropriate controls are as indicated. **C**. Basal (in solution) and stimulated (on DOPS membranes) GTP-hydrolysis activity of Dynamin1 and VL4 mutant (Dyn1 F579A). Data represent the mean \pm SD of three independent experiments.

4.2.3 Membrane fission using Supported Membrane Templates

Using a facile and high throughput assay previously developed in the lab^{80,125}, that allows formation of an array of tubes pinned on passivated glass surface, we tested dynamin-catalysed membrane fission. These tubes mimic tubular intermediates at the neck of CCPs that dynamin finally acts on during clathrin-mediated endocytosis. Dynamin1 in presence of GTP and its co-factor MgCl_2 displays robust fission of these templates made

from 100 mole percent DOPS. When tested under similar conditions, Dynamin1 F579A showed equally robust fission activity on these templates. For a finer analysis, we recorded this reaction in real-time and compared time-lapse frames to bring out differences in kinetics and the extent of membrane fission but no significant difference was observed between the two proteins (Figure 4.4).

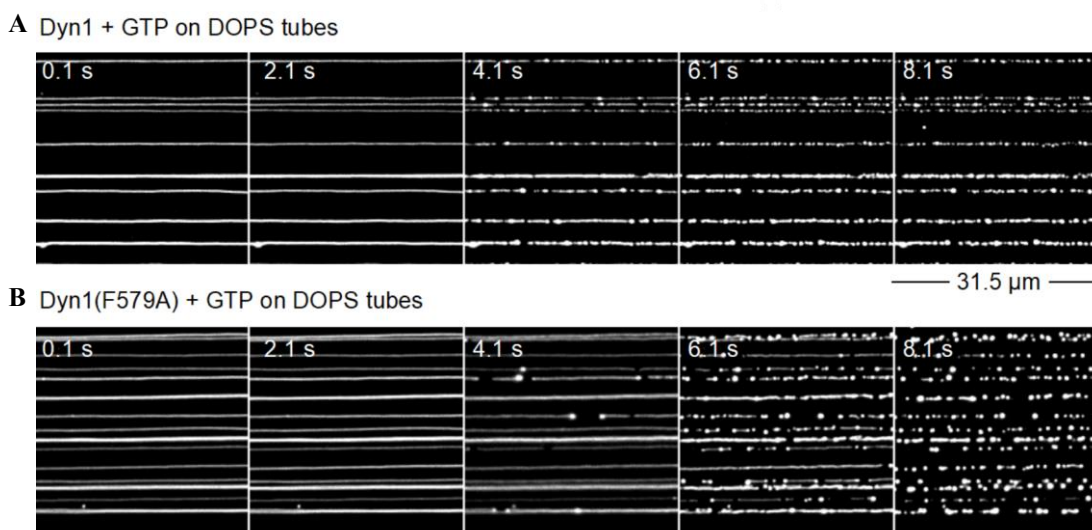


Figure 4.4 Dynamin mediated membrane fission on highly anionic membranes.

Time-stamped frames from a timelapse movie showing fission of supported membrane nanotubes with **A.** Dyn1 and **B.** the VL4 mutant Dyn1 F579A in the presence of GTP.

4.3 Discussion

In bulk assays where a hundred-fold excess of liposomes to that of the protein concentrations were used, dyn1 F579A showed efficient binding to highly anionic membranes when compared with the WT protein. Biochemical analysis revealed that the GTP-hydrolysis activity of Dyn1 F579A is also comparable to Dyn1. To test Dyn1 F579A membrane fission, a fluorescence microscopy-based assay was used alongside GTP and co-factors and fission of model membranes *viz.* an array of supported membrane nanotubes that mimic the neck of CCPs was monitored. In such fission assays performed on highly anionic membranes, Dyn1 F579A showed robust fission efficiency. However, dynamin is best known for its function during fission of clathrin-coated vesicles at the plasma membrane, where it encounters significantly lower content of negative charge as compared to membranes containing 100 mole percent DOPS. While these results rule out global defects and definitively ascertain proper folding and functioning of Dyn1 F579A, they fall short of uncovering the relevance of VL4 in dynamin functions in a physiologically relevant scenario.

Chapter 5

**PROBING THE SIGNIFICANCE OF VL4 IN
DYNAMIN-MEDIATED FISSION ON
MEMBRANES OF PHYSIOLOGICAL
PHOSPHOLIPID COMPOSITION**

5.0 Probing the significance of the novel VL4 in dynamin-mediated fission on membranes of physiological phospholipid composition

Physiological functions of dynamin are best understood in the context of release of clathrin-coated vesicles from the plasma membrane. In order to analyse dynamin1 F579A functions on a physiologically relevant membrane composition, we used membranes made from 15 mole percent DOPS and 1 mole percent PI(4,5)P₂ or PIP₂ with the bulk of the membrane being made of the zwitterionic phospholipid DOPC. This proportion and nature of lipids closely mimics the phospholipid composition of the plasma membrane.

5.1 Dynamin1 F579A shows reduced membrane binding affinity in bulk assays

To test if VL4 is critical for dynamin-membrane binding, we analysed the membrane binding of the VL4 mutant using the facile, sensitive and quantitative assay PLiMAP as previously described^{122,123} (See section 2.6 for details). Here, PLiMAP was performed with purified proteins using liposomes made of physiologically relevant relative concentrations, and doped with one mole per cent of the bifunctional lipid probe. A binding isotherm for dynamin1 WT and F579A was obtained by subjecting them to independent reactions with increasing concentrations of PIP₂ to arrive at an estimate of membrane binding determinants such as apparent affinity (K_d) and total binding sites (B_{max}).

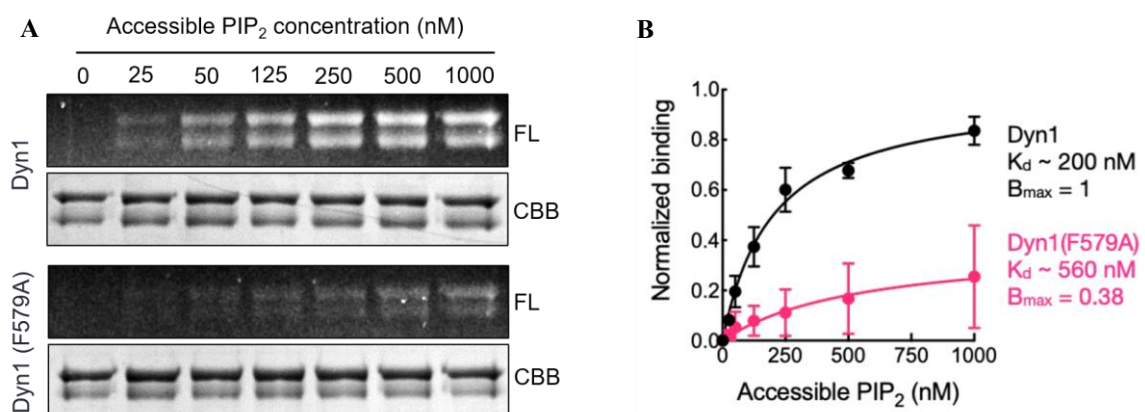


Figure 5.1 Dynamin binding analysed on physiological membranes in bulk assays.

A. Representative PLiMAP gel showing in-gel fluorescence (FL) and Coomassie brilliant blue (CBB) staining of Dyn1 and the VL4 mutant on liposomes with 15 mole percent DOPS and 1 mole percent PIP₂. **B.** Quantification of data in A. Band intensities were fit to gaussians and normalised amplitude was plotted after subtracting the background intensities from each. Data represent the mean \pm SD of three independent experiments.

We saw that on these membranes mimicking the plasma membrane composition, dynamin1 F579A showed significantly deterred membrane binding capability. The observed K_d for dynamin1 F579A was ~3 fold lesser than that observed for dynamin1. In addition, it was seen that the B_{max} that is a reporter for total binding sites between the substrate and the ligand had also reduced by ~2.5 fold (Figure 5.1). This led us to hypothesize that VL4 forms an additional membrane binding site in the dynamin PHD, over the previously known VL1. This result showed for the first time that VL4 is necessary for dynamin-membrane binding.

5.2 Dynamin1 VL4 tip mutants with perturbed loop hydrophobicity show curvature sensitive defects in membrane binding and self-assembly

Prior studies examining the binding of peripheral membrane proteins have suggested that the dissociation constant (K_d) signifies the interaction strength between particular protein residues and lipids, whereas the maximum binding capacity (B_{max}) is influenced by the presence of both the interacting lipid abundance and membrane defects that assist in incorporating hydrophobic residues into proteins¹²⁸. Furthermore, membranes with high curvature exhibit a greater prevalence of membrane defects¹²⁹. Through MD simulations, it has been demonstrated that, unlike VL1, VL4 does not engage in a direct interaction with PIP₂¹⁰³. This prompts the question whether VL4's capability to insert into membrane defects might lead to an allosteric stabilization of dynamin on the membrane. If this hypothesis holds true, then the F579A mutation could potentially render dynamin binding more sensitive to membrane curvature. Therefore, to better understand the binding defects observed for dynamin1 F579A and obtain a clearer picture of the membrane-binding reaction, we resorted to spatiotemporally resolved fluorescence microscopy-based assays. We tested dynamin-membrane binding using supported membrane tubes (SMrT) on PEG-cushioned glass coverslips inside a flow cell as described earlier^{80,125} (See section 2.7). Here, tubes were made out of a lipid mix containing 15 mole percent DOPS and 1 mole percent PIP₂ with the bulk of the membrane being DOPC. In addition, one mole percent of a fluorescent probe DHPE-TexasRed was doped into this mix for visualisation in microscopic assays. It has been previously reported that N-terminal GFP-fusion of dynamin is inactive and C-terminal fusion is partially active. Therefore, we used dynamin extrinsically labelled with small fluorophores (here, Alexa488 C5-maleimide, see section 2.2 for more details).

Supported membrane tubes were formed with the aforementioned lipid mix in a flow-cell chamber and then dynamin1^{Ax488} was flown-in and allowed to incubate for 10 minutes. Excess protein was then washed off with buffer and images were acquired. Bound dynamin1 showed discrete foci representing protein scaffolds on the membrane that correlated with a dip in membrane fluorescence indicating constriction of the underlying membrane tube, imposed by the protein scaffold. Dynamin1 scaffolds on the membrane were observed on all sampled tubes, which were ranging from 10-100 nm in radius. Dynamin1 showed little to no curvature preference under this regime. When dynamin1-F579A^{Ax488} which has reduced VL4 hydrophobicity was tested under similar conditions, significant defects in membrane binding were uncovered. One, dynamin1-F579A^{Ax488} showed dramatically lower number of foci on membrane tubes. Two, the observed foci were drastically low in occurrence even on tubes where they were found. Since dynamin binding to membrane and forming scaffolds that are observed as fluorescent foci is a stochastic process, we analysed the probability of finding at least one dynamin puncta correlated with the membrane and plotted it as a function of tube radius. This analysis revealed a steeper curvature-dependence in dynamin1 F579A (Figure 5.2). Moreover, the CMT-associated mutant M580T that reduces VL4 hydrophobic character even more dramatically, showed very similar results in microscopic assays when membrane binding was plotted as a function of tube radius.

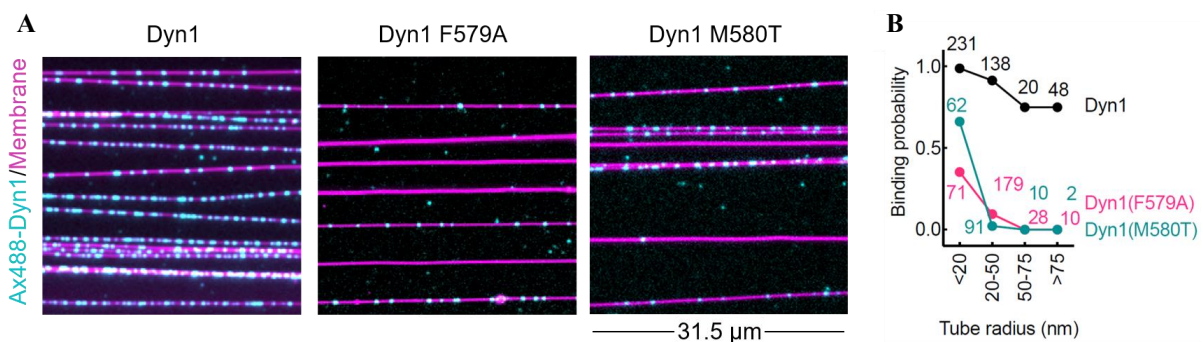


Figure 5.2 Dynamin binding to physiological membranes in microscopic assays.

A. Representative micrographs showing dynamin1 and VL4 mutants scaffolds (cyan) on supported membrane tubes (magenta) of physiological phospholipid composition. **B.** Quantification of data in A. Binding probability is plotted as a function of tube radius. Numbers indicate the number of tubes sampled for each bin.

5.3 Dynamin1 VL4 tip mutants with reduced loop hydrophobicity but not altered loop charge, show curvature sensitive defects in membrane fission

To test fission activity, dynamin1 mixed with GTP and MgCl₂ was flown onto pre-equilibrated supported membrane tubes. Images of fields recorded before flowing in dynamin were compared to the images captured after flowing in dynamin, to estimate fission activity. SMrTs represent an array of infinite substrate for dynamin function. The fission reaction proceeds as a stochastic process and several events can be seen on a single tube. Fission efficiency was plotted as the probability of finding at least one cut per tube over the total number of sampled tubes, as a function of tube radius. While dynamin1 showed robust fission of tubes with no curvature dependence within the sampled range of tube radii, dynamin1 F579A showed a steep decline in activity above tubes of 15nm radius. Dynamin1 M580T when tested under similar conditions showed the same results as dynamin1 F579A (Figure 5.3). This result showed that reduced VL4 hydrophobicity leads to partial defects in membrane fission and render dynamin functions more sensitive to membrane curvature.

Some dynamin-like proteins have been shown to have lysine residues that are critical for binding to negatively charged membranes. The hydrophobic tip of VL4 is also flanked by two lysines. To test whether lysine-mediated electrostatic interactions are critical for dynamin function, we cloned a mutant K583A and tested it in fission assays. On supported membrane tubes made from physiologically relevant lipid composition, dynamin1 K583A showed robust fission unlike the mutants that altered VL4 hydrophobicity (data not shown as it coincides with Dyn1 WT on the plot). Therefore, we concluded that while disruption of the hydrophobic character of this tip render dynamin defective in membrane fission, alteration of charge on the loop edge that might hamper headgroup interactions, does not apparently affect dynamin function. This result strengthened the idea that membrane insertion of the VL4 hydrophobic tip is critical for dynamin functions.

5.4 Dynamin2 functions are more sensitive to membrane curvature than Dynamin1

The Charcot-Marie-Tooth neuropathy is linked to mutations in dynamin2. Since dynamin2 is the ubiquitously expressed dynamin paralog which is also found in muscle tissue where the disease manifests, we tested dynamin2 F579A and M580T in fission assays in comparison with dynamin2. It has been shown earlier that dynamin2 is inherently different from dynamin1 in its capacity to bind and sever membranes such that it has a lesser affinity for the membrane,

has higher curvature dependence, and has a lower GTP-hydrolysis activity. Our results confirmed that dynamin2 indeed showed a steeper curvature preference and showed fractional probability to sever tubes only upto 20 nm radius whereas dynamin1 showed robust fission of tubes of similar sizes. Moreover, dynamin2 F579A and M580T showed no fission of similar sized tubes, emphasizing that dynamin2 might be more susceptible to loss of function in such mutations during disease pathology (Figure 5.3).

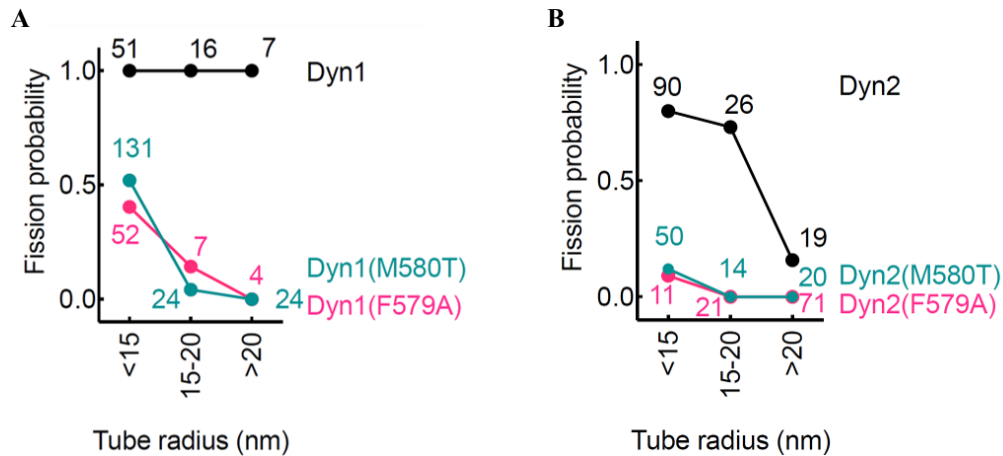


Figure 5.3 Comparative analysis of Dyn1/2 fission activity on physiological membranes.

Fraction of cut tubes observed over total number of sampled tubes (indicated as numbers) shown as fission probability across a range of tube radii with **A.** Dynamin1, & **B.** Dynamin2.

5.5 Discussion

Binding and fission assays unambiguously show, for the first time, that VL4 is critical for dynamin function and that any alteration, even subtle, in the hydrophobic character of VL4 leads to partial loss of function affecting membrane binding and fission, both.

It is unsurprising that a mutant in the PHD results in impaired membrane binding. However, it is rather interesting that the result does not only arise from a change in the binding affinity of the protein but also from a loss in total available binding sites consequentially displaying a marked drop in the B_{\max} of the reaction. While the apparent K_d of Dyn1 F579A for PIP₂ binding drops by almost a third, the B_{\max} also drops by about 2.5-fold in comparison to Dyn1. Although, given the available binding sites on the lipids in both the reactions remain the same, a drop in B_{\max} must reflect from a change in available binding sites on the protein. This suggests that VL4 presents as an additional site on the dynamin PHD for membrane-binding.

It is important however to note that while reduced VL4 hydrophobicity renders dynamin less effective in membrane-interaction and consequently fission, however, does not completely abrogate its membrane-binding.

PHD-membrane engagement frees the stalk for stalk-stalk crosstalk and dynamin forms oligomers on the underlying tube in a spiral manner with interfaces between two rungs associated with each other. This intricate self-assembly is a consequence of stable PHD-membrane engagement. A PH-domain that only loosely associates with the membrane may not let go of the autoinhibition it exerts on the molecule by binding to the stalk. A low K_{on} for Dyn1 F579A is already apparent from the bulk membrane binding assays (PLiMAP) where equilibrium binding is analysed and no-washing off of excess protein is involved. Furthermore, since the number of Dyn1 F579A foci observed per tube in binding assays done with SMrTs in the case of the mutant protein were far fewer than dynamin1 where present at all, it indicates that VL4 is required for stable engagement of dynamin PHD with the membrane. Failing this, the protein likely loosely binds the membrane and displays high K_{off} , thus falling-off easily as opposed to the WT protein, upon washing. In fact, these results corroborate with previous findings showing that prevalence of membrane defects on highly curved membranes can indirectly enhance the stability of membrane insertion of hydrophobic patches on peripheral membrane binding proteins, therefore allosterically stabilising dynamin on thinner tubes and manifesting as higher curvature sensitivity in protein functions.

It is rather intuitive that dynamin mutants that show defects in membrane binding would also show lack of fission, as membrane-binding is a pre-requisite for membrane fission. In the minimal setup used for these assays, the protein's ability to recruit to the membrane relies solely on its engagement with phospholipids in the underlying bilayer. However, during clathrin-mediated endocytosis, dynamin is known to be recruited to endocytic pits by protein-protein interactions between dynamin's PRD and adaptor proteins' SH3 domains. The assays setup in the present case, however, bypass the requirement for other molecules such as adaptor proteins in the cell that might act to bring dynamin to its site of action prior to PHD-membrane engagement being realized. In such a scenario, it remains unclear if VL4-membrane engagement is really significant for dynamin-mediated membrane fission.

Chapter 6

**COMPARATIVE ANALYSIS OF VARIABLE
LOOP EFFECTS ON DYNAMIN FUNCTIONS**

6.0 Comparative analysis of variable loop effects on dynamin functions

Dynamin assembly leads to membrane constriction (Figure 6.1). Fission proceeds upon GTP-hydrolysis induced conformation changes, due to progressive constriction and consequential severing of the membrane underlying the dynamin scaffold¹²⁵.

Mechanistically, hydrophobic loop insertion is thought to lower the bending rigidity of the membrane, thus making it more amenable to fission^{127,103}. However, experimental evidence corroborating this notion is very limited. It is well-known that the Isoleucine residue at the tip of VL1 i.e., I533 inserts into the membrane bilayer and facilitates stable dynamin-membrane binding. Counterintuitively, however, VL1 mutant Dyn1 I533A has been demonstrated to achieve fission in shorter time scales than Dyn1 WT⁸⁰. As in, if allowed to self-assemble on a membrane nanotube and subsequently supplied with GTP, Dyn1 I533A in fact takes a shorter time to achieve fission, than Dyn1 WT. This parameter is better described as the fission time. This indicates that VL1 perhaps inhibits fission. A fine analysis of intermediates formed during this reaction also show that I533A facilitates dynamin-induced membrane constriction⁹⁴. Notes of this analysis are described ahead. In order to underline commonalities and differences in the effect of variable loop membrane insertion in dynamin function, we analysed intermediates formed by VL1 and VL4 mutants in close detail, as previously described^{80,125}.

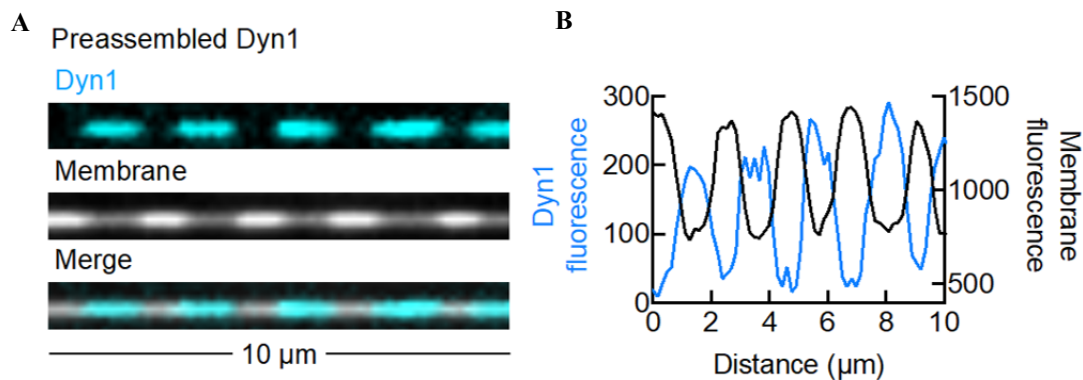


Figure 6.1 Dynamin1 scaffold constricts the underlying membrane tube.

A. Representative micrographs and **B.** line profile of the same, showing Dynamin1 scaffolds (cyan foci) that constrict the underlying tube. Dimmer membrane fluorescence under the Dyn1 foci indicates thinning of the tube representing dynamin assembly-induced constriction.

6.1 Membrane fluorescence correlated to tube radius enables study of intermediates formed during real-time analysis of dynamin-catalysed membrane fission

Principally, the fluorescence intensities of diffraction-limited, membrane-bound objects are proportional to the net membrane surface area. The supported membrane tube assays are performed using a wide-field epifluorescence microscope and therefore, total intensity of a tube can be directly correlated to its size. To equate the fluorescence intensity to tube sizes, we first derive a correlation function, by plotting the intensity per unit area of the planar supported lipid bilayer formed near the source as described earlier. The slope of this curve provides a calibration constant k_l which can be used to derive surface area of the tube, which can be in turn be used to estimate the radius of the tube, as given in the following equations:

Because, $area = (I/k_l)$

Therefore, $radius = area/2\pi l$

or directly, $radius (nm) = (I/k_l) * 1000/(2\pi l)$

Where k_l is the calibration constant described above, 'I' is the integrated intensity of a tube and l is the length of tube from which the fluorescence intensity is collected. Since the scaling factor obtained from the microscope in our setup accounts for conversion of pixels to micro meter, a factor of 1000 is used for conversion to obtain nano meter tube radii.

Furthermore, tube radius estimated before dynamin assembly can be used to arrive at a direct relationship between tube intensity and radius. A plot of maximum tube intensity as a function of tube radius provides the calibration constant k_2 which can thereon be used to obtain radius of tubes by directly converting pixel intensity to approximate sizes.

Dynamin mediated membrane fission proceeds in a manner such that the dynamin scaffold progressively constricts the underlying tube upon self-assembly and GTP-hydrolysis, and drives the underlying bilayer to critical dimensions leading to spontaneous fission^{80,125}. This process is thought to progress through a hemi-fission intermediate stage where only the outer monolayer remains fused whereas the inner monolayer is discontinuous or severed¹³⁰.

Since tube fluorescence is directly proportional to the tube radius, the region under the dynamin scaffold appears dimmer and further dims upon GTP-hydrolysis, before proceeding to fission (Figure 6.2A). By monitoring these reactions in real-time, we record progressive change in tube intensity upon dynamin self-assembly and fission. The radius of tube underneath

as scaffold is termed ‘scaffolded’ (magenta) tube radius and the super constricted radius of tube attained after GTP-hydrolysis just prior to fission is termed ‘pre-fission’ (cyan) tube radius, as shown in Figure 6.2A and Figure 6.2B. These parameters enable us to arrive at mechanism of dynamin function by monitoring changes in membrane fluorescence over-time, and distinguish mechanistic defects that might arise in upon mutational perturbation.

6.2 VL4 facilitates whereas VL1 inhibits dynamin-mediated membrane fission

It has been estimated by simulation based enquiry that membrane's resistance to bending is reduced upon PHD binding¹⁰³. This outcome arises likely due to a localized increase in the flexibility of the fatty acyl chains in the lipids and a decrease in membrane thickness. Dynamin1 assembly on the membrane imposes the inner dimensions of the dynamin scaffold on the tubes whose mean radius is ~10 nm (Figure 6.2C), in absence of nucleotides. We show that VL1 aids constriction as the VL1 tip mutant (Dyn1 I533A) cannot adequately constrict the membrane resulting in a wider scaffolded tube of mean radius ~13.8 nm (Figure 6.2C). On the contrary, our results demonstrate that VL4 inhibits constriction, as the VL4 tip mutant (Dyn1 F579A) results in a thinner scaffolded tube than Dyn1, with a mean radius of ~7.5 nm (Figure 6.2C). MD simulations also show that in the VL4 mutant (Dyn1 F579A), VL1 dips deeper into the membrane¹⁰³, indicating that VL1 constricting functions could be enhanced in the VL4 mutant, Dyn1 F579A. Findings from our experiments substantiate this hypothesis.

GTP hydrolysis propels further constriction of the scaffolded tube until it reaches a critical pre-fission intermediate with a radius of ~5 nm before fission occurs with Dyn1. Surprisingly, even upon GTP-hydrolysis, Dyn1 I533A exhibits a wider pre-fission intermediate than Dyn1 with a mean radius of ~6.4 nm, while Dyn1 F579A displays a narrower pre-fission intermediate than Dyn1 with a radius of ~3.6 nm (Figure 6.2C).

Notably, in case of Dyn1, the tube must constrict to a thinner dimension before it undergoes fission. However, in case of Dyn1 I533A, when VL1 functions are inhibited, fission is achieved with a less pronounced degree of constriction at a wider dimension of the pre-fission intermediate. These results point to a mechanism where VL1 aids in membrane constriction, but unexpectedly hinders fission. Conversely, VL4 has the opposite effect, hindering constriction but facilitating fission as in case of Dyn1 F579A where VL4 functions are inhibited, the tube hyper constricts before fission ensues. This may seem counterintuitive as mechanisms that aid in narrowing the scaffold would be expected to promote fission. Yet, it

underlines the intricacies of regulatory mechanisms manifested by molecular dynamics in membrane fission. Moreover, this further emphasizes that VL4 is critical to promote fission.

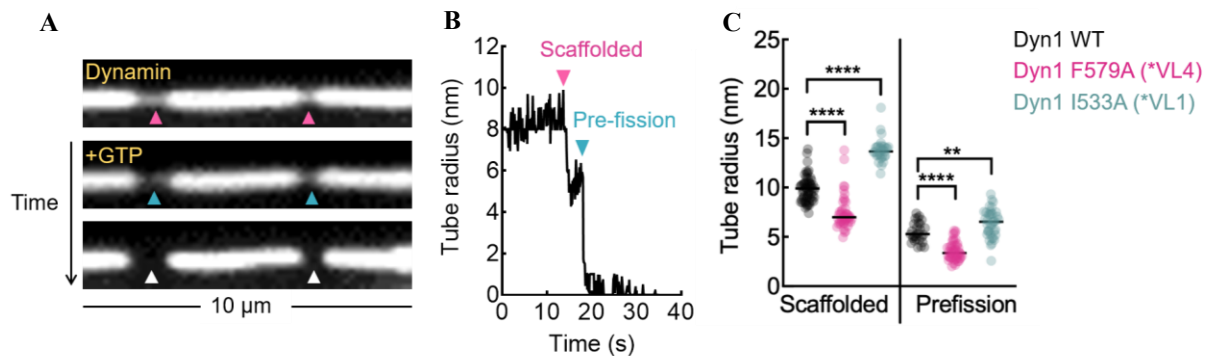


Figure 6.2 Dynamin1 self-assembly and GTPase induced constriction leading to fission.

A. Representative micrographs of dynamin assembled on membrane undergoing fission over time upon introduction of GTP. **B.** Tube radius changes under dynamin scaffold progressing towards fission. In A and B, magenta indicates scaffolded and cyan indicates pre-fission intermediates. **C.** Comparative analysis of scaffolded and pre-fission tube radii between tip mutants of VL1 (I533A) & VL4 (F579A) showing distinct effects on Dyn1 functions.

6.3 Discussion

It is apparent from these results that variable loop insertion in the underlying bilayer can have distinct and opposite effects. In this case especially, coupled with the results obtained from structural modeling where we showed that VL insertion into the bilayer is exclusive i.e., at any one time, only one variable loop forms the preferred membrane anchor for each dynamin molecule within a scaffold. In the ensemble however, VL1 and VL4 form the most preferred membrane anchors. That VL1 insertion is exclusive suggests that an inhibition mechanism by which this negative allostery in VL insertion is governed must be in place. However, the underlying molecular mechanisms that govern this functional specificity and insertion selectivity remain elusive but an intriguing hypothesis is that the VLs operate akin to gears within the dynamin fission apparatus. Much like how gears modulate the operational capacity and catalytic output of a machine, the efficiency of fission by dynamin as a molecular machine is likely to be finely modulated based on the nature and extent of membrane engagement by different variable loops at any time. To gain a more profound understanding of these effects, future atomistic MD simulations of the fission process, the analysis of membrane intermediates formed during extreme narrowing, and structural modeling of mutant dynamin scaffolds are likely to provide valuable mechanistic insights.

Chapter 7

**RECONSTITUTING DYNAMIN FUNCTIONS IN
A NATIVE-LIKE CONTEXT**

7.0 Reconstituting dynamin functions in a native-like context

The assays mentioned previously have notable limitations since they heavily depend on dynamin's lipid-binding capability to recruit it to the membrane. In the cellular milieu, dynamin relies on intricate, multivalent interactions involving both lipids and endocytic proteins as described in *Chapter 1*. Specifically, the PHD binds to PIP₂, while the PRD engages with various SH3 domains present in endocytic proteins that capture cytosolic dynamin at the endocytic pits⁵⁷. These collective interactions are crucial for dynamin's recruitment to the membrane. To mimic these complex interactions in our experiments, we endeavoured to enlist adaptor proteins (those containing BAR domains) that bind to dynamin onto supported membrane tubes. Regrettably, our attempts to recruit partners of Dyn1, such as amphiphysin1 and endophilin, proved unsuccessful, as these proteins exhibited minimal affinity for templates containing 1 mole percent PIP₂ and 15 mole percent DOPS.

As an alternative approach, we turned our attention to Amphiphysin2 or BIN1 (bridging integrator 1, also known as Box-dependent myc-interacting protein 1), particularly isoform eight. This isoform features a positively charged PI region that exhibits a high-affinity binding to PIP₂. Additionally, it possesses an SH3 domain that interacts with dynamin and plays a pivotal role as a binding partner in clathrin-mediated endocytosis (CME)^{110,118,131–133}.

7.1 A dynamin binding partner BIN1 (Amphiphysin2) is membrane-active

BIN1 (also known as Bridging-integrator1 or Amphiphysin2) exhibits membrane-active behaviour. When we introduced BIN1-GFP to SMrTs containing 1 mole percent PIP₂ and 15 mole percent DOPS, it promptly bound to the nanotubes. BIN1-GFP displayed two distinct patterns: on some nanotubes, thinner ones specifically, it exhibited even distribution (marked by the box with a dotted line and corresponding fluorescence profiles in Figure 7.1), while on others or thicker tubes, it formed discrete foci (highlighted by the box with a solid line and associated fluorescence profiles in Figure 7.1). These foci were associated with reduced membrane fluorescence, indicating constriction of the underlying tube.

Although BIN1 is well-known for its ability to induce tubulation of planar membranes¹³³, its propensity to organize into active membrane scaffolds on tubes had not been previously documented. Consequently, we decided to further investigate into this phenomenon. To assess the uneven distribution of BIN1 along the tube's length, we calculated the coefficient of variation (COV) of BIN1-GFP fluorescence. The COV increased as the tube radius expanded.

Conversely, the membrane density of BIN1-GFP, determined by dividing the average BIN1-GFP fluorescence by the average membrane fluorescence, decreased with an increase in tube radius. These findings collectively suggest that as the tube size increases, BIN1 shifts from forming extended, continuous scaffolds to smaller, discrete units, likely due to limitations in protein density on the membrane.

By comparing the radius of the scaffolded tube to the original tube radius, we clearly observed BIN1's capacity to constrict the tube. Tubes initially measuring around 10 nm in radius maintained their size, whereas tubes with an initial radius of approximately 30 nm were thinned down to about 12 nm. These measurements closely match the reported limit of 14 nm obtained from cryo-electron microscopy examinations of large vesicles tubulated by BIN1¹³⁴. However, the radius of the scaffolded tube exhibited only a relatively shallow dependence on the initial tube radius, suggesting that BIN1 scaffolds possess a degree of plasticity or adaptability and can conform to the dimensions of the underlying tube.

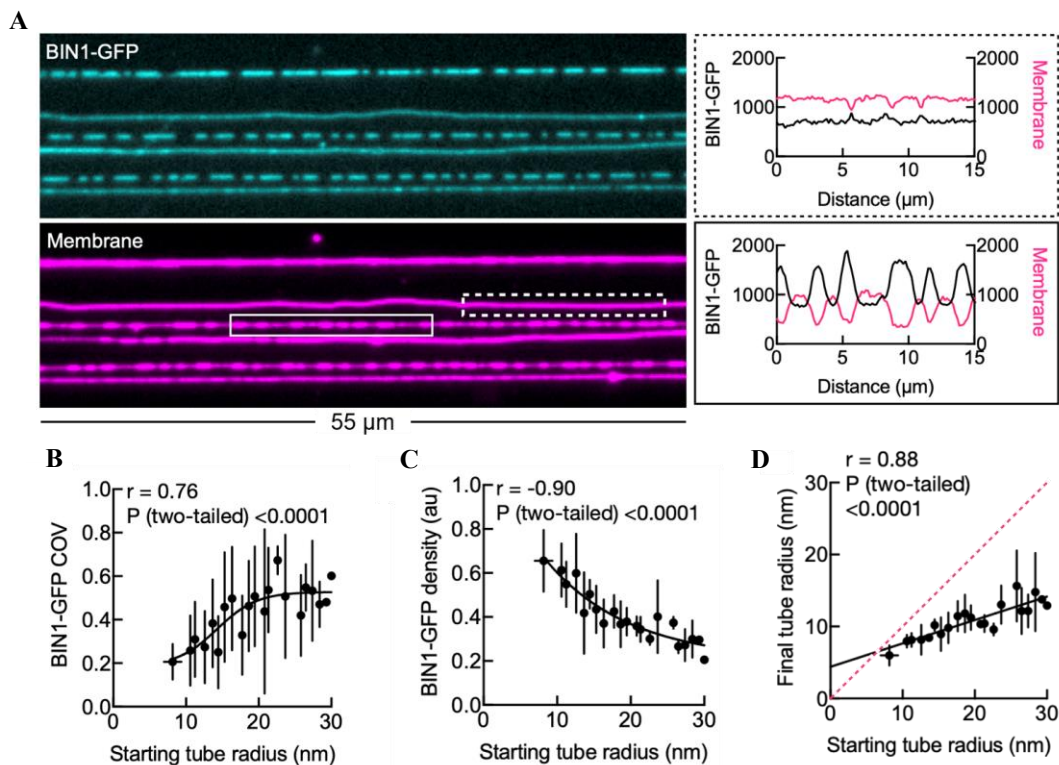


Figure 7.1 BIN1 or Amphiphysin2 is membrane active.

A. Representative micrographs of BIN1-GFP assembled on tubes. Dotted box shows a thinner tube with continuous BIN1 fluorescence and solid box shows thicker tube with discrete BIN1 foci. **B.** The coefficient of variance of BIN1-GFP fluorescence, increasing as a function of starting tube radius. **C.** The BIN1-GFP density, decreasing as a function of starting tube radius. **D.** Correlation of initial (pink) and final (black) tube radius upon BIN1-assembly.

7.2 BIN1 recruits both Dynamin1 and Dynamin1 F579A to membrane nanotubes

Given these characteristics, it appears that BIN1-coated membrane nanotubes offer an ideal framework for exploring the functions of dynamin1 in a more physiologically relevant context. BIN1 scaffolds display a high local density of SH3 domains and possess the capability to constrict underlying tubes with various sizes to a narrow range with a mean radius of about 12 nm. This unique property is expected to: i) recruit dynamin via its PRD to the displayed SH3 domains thereby getting it on the membrane despite lipid-binding defects, and ii) alleviate the pronounced dependence on membrane curvature observed with Dyn1 F579A during membrane fission processes as the BIN1 scaffold itself narrows down the tube to dimensions where Dyn1 F579A is active.

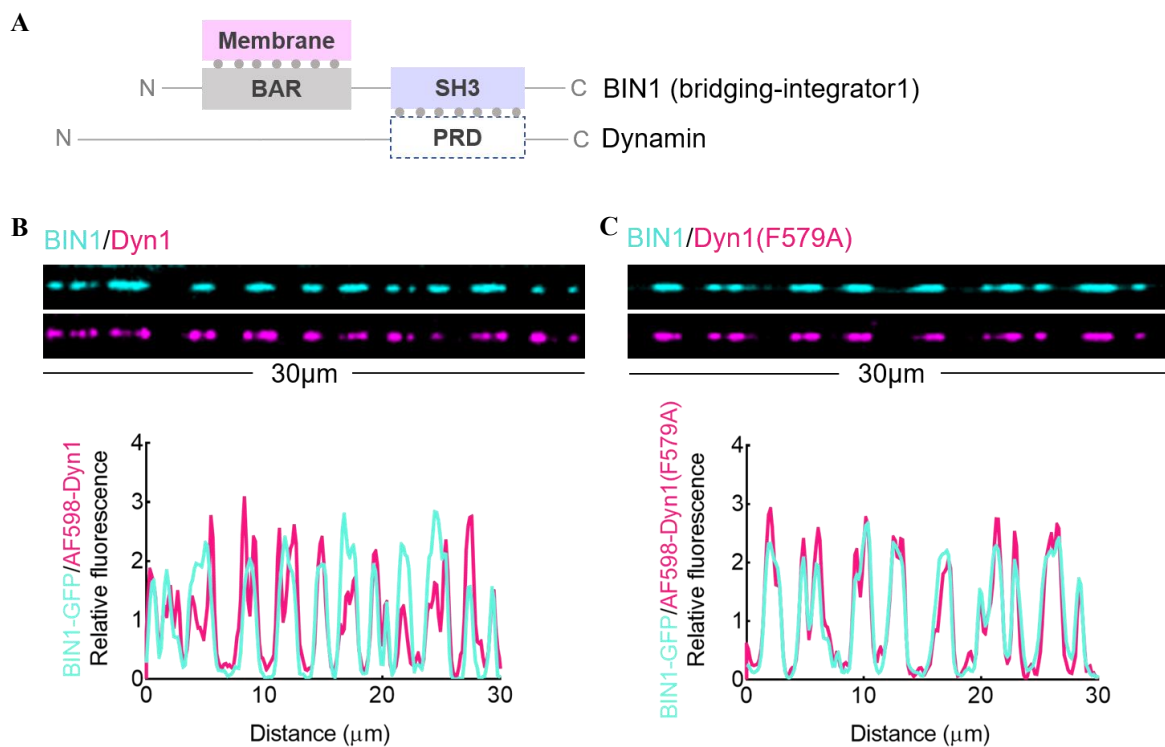


Figure 7.2 BIN1 scaffolds stably recruit Dyn1 F579A on the membrane.

A. Schematic depicting strategy for recruitment of dynamin on the membrane. Using sequential recruitment as shown in **A**, BIN1 captures dynamin efficiently on the membrane as seen in representative micrographs of **B**. Dynamin1 (top) or **C**. Dynamin1 F579A (top) captured on BIN1 scaffolds. Bottom panel in **B** and **C** shows corresponding line profiles of BIN1 and dynamin fluorescence.

To validate dynamin's interaction with BIN1 through SH3-PRD associations on membrane nanotubes, particularly in light of the partial C-terminal truncation of the PRD observed in our recombinant dynamin preparations (detailed in *Chapter 2*), we formed nanotubes, flowed in BIN1-GFP and allowed it to bind, subsequently washing off excess protein. Then, we introduced fluorescent dynamin in the flow cell. The fluorescence patterns of Dyn1 F579A and BIN1-GFP coincided precisely, indicating that the BIN1 on tubes effectively recruits Dyn1 F579A (Figure 7.2). Consequently, it appears that the partial C-terminal truncation of the PRD does not have a significant impact on dynamin's ability to interact with BIN1's SH3 domain.

7.3 Dynamin1 F579A shows dramatic lack of fission on BIN1 coated-tubes

With Dyn1 F579A stably recruited to membrane nanotubes through multivalent lipid-protein interactions, mirroring a native-like context, we proceeded to investigate membrane fission by dynamin. To do so, we assessed dynamin's functions in the presence of GTP on membrane nanotubes coated with BIN1. In these experiments, we focused solely on the membrane fluorescence to improve temporal resolution, as our prior findings established that BIN1 is distributed either uniformly along narrow membrane tubes or localized as discrete scaffolds, each of which corresponded to reduced tube fluorescence (Figure 7.1).

The introduction of Dyn1 with GTP on BIN1-coated membrane nanotubes led to membrane fission. This fission was apparent on nanotubes uniformly coated with BIN1, as well as on those exhibiting localized BIN1 scaffolds constricting the tube underneath (Figure 7.1). The kinetics of bulk fission, mediated by dynamin1 and estimated by counting the number of cuts observed over time across several tubes within the microscope's field of view, was slightly slower on BIN1-coated tubes (approximately 1.6 cuts per second) compared to tubes without BIN1 (~4.8 cuts per second). This difference might be attributed to the presence of BIN1, which competes for binding to the available PIP₂ necessary optimal membrane engagement by dynamin. Time-lapse imaging of tubes featuring localized BIN1-dependent constrictions ascertained that fission in fact occurred within the BIN1 scaffold and not elsewhere on the tube, indicated by the splitting of the dimmer constricted region on the tube upon dynamin action (Figure 7.3B).

Notably, flowing Dyn1 F579A with GTP did not induce any fission of BIN1-coated membrane nanotubes under identical conditions (Figure 7.3A). In fact, not a single membrane fission event was observed on tubes in this case (Figure 7.3). Furthermore, when correlating

the likelihood of fission with the initial tube size, it became evident that this mutant was deficient in inducing fission across a range of tube sizes (Figure 7.3C).

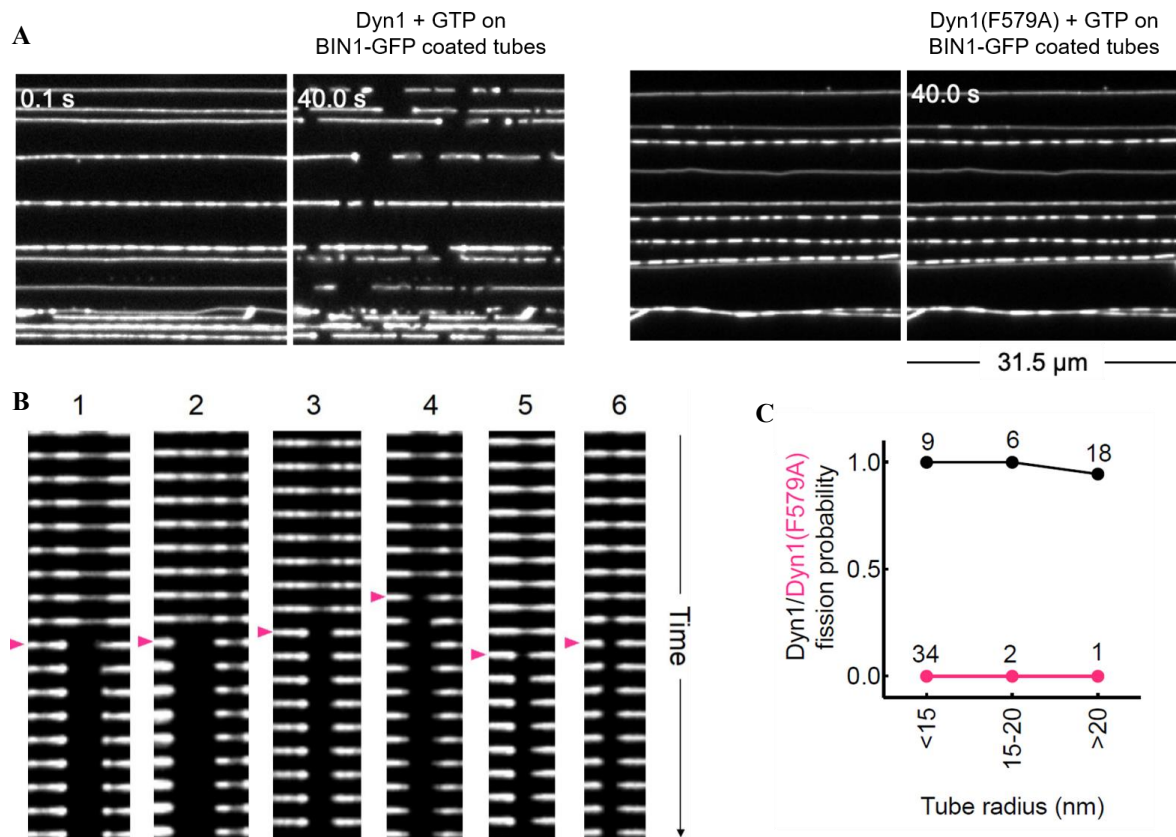


Figure 7.3 Dyn1 F579A is incapable of inducing fission of BIN1-coated tubes.

A. Representative fluorescence micrographs showing the effect of addition of Dyn1 (left) and Dyn1 F579A (right) with GTP and $MgCl_2$ to BIN1-coated membrane nanotubes. **B.** The panel shows 6 independent fission events by dynamin1 on BIN1-coated tubes. In both A and B, only membrane fluorescence is shown. Dim regions correspond to BIN1-scaffolds. All six montages indicate that the site of fission is confined within the BIN1 scaffold, which is apparent because the dimmer constricted region on the nanotube undergoes severing. The time frame when fission is observed is marked by magenta arrows. **C.** Probability of fission observed with Dyn1 (black) and Dyn1(F579A) (magenta) as a function of starting tube radius. Total number of tubes sampled in each bin are indicated as numbers within the plot.

7.4 Discussion

We anticipated that the deficit in membrane binding and fission observed with Dyn1 F579A could potentially be rescued by incorporating SH3-PRD interactions by BIN1 as it could ensure dynamin recruitment to the membrane despite partial lipid-binding defects in

Dyn1 F579A. BIN1 scaffolds display a high local concentration of SH3 domains, and as demonstrated in the results presented here, they also possess the ability to constrict membrane tubes to a size conducive to fission. Our results showed that BIN1 scaffolds indeed acted as potent facilitators of dynamin's recruitment to the membrane in this context.

It's worth noting that previous reports have suggested that an excess of BAR domain proteins, such as endophilin and amphiphysin, can inhibit dynamin functions, likely by forming mixed scaffolds that hinder dynamin's G-domain interactions necessary for its stimulated GTPase activity^{135,136}. However, in our experimental setup, we designed assays that allowed BIN1 to initially form scaffolds and then recruit dynamin sequentially, ruling out the possibility of forming mixed scaffolds. To ensure that dynamin self-assembles within the BIN1 scaffold to initiate fission, we washed off excess BIN1 before introducing dynamin into the reaction chamber. This sequential addition approach closely mimics the cellular scenario where endocytic proteins are known to arrive before dynamin, to facilitate the fission of clathrin-coated pits^{57,110}, although, alternate models proposing cooperative but not necessarily sequential, recruitment of endocytic proteins and dynamins have also been put forth¹³².

Surprisingly, despite Dyn1 F579A binding effectively to BIN1 scaffolds, it exhibited a remarkable failure in inducing fission. One key factor at play here is that BIN1 likely competes with dynamin for binding to PIP₂, and the slightly reduced affinity of Dyn1 F579A for PIP₂ may impact its ability to actively engage with the membrane in presence of a competing binding partner such as BIN1.

Chapter 8

**PROBING THE SIGNIFICANCE OF VL4 IN
CELLULAR FUNCTIONS OF DYNAMIN**

8.0 Probing the significance of VL4 in cellular functions of dynamin

Our results from bulk liposome binding assays as well as microscopy-based supported membrane nanotube assays have already demonstrated that VL4 is critical for dynamin functions. Although, as discussed in the previous chapter, we reconstitute dynamin functions in a native-like context by recruiting dynamin to the membrane via protein and lipid-based interactions closely mimicking cellular conditions, it remained to be tested whether the defects we observe in reconstitution-based biochemical assays would manifest in the far more complex and intricately regulated environment of a cell.

8.1 Dynamin1 F579A and M580T impair clathrin-mediated endocytosis in cells

During CME, dynamin is recruited to the necks of clathrin-coated pits during late stages to catalyse fission, leading to the release of clathrin-coated vesicles. The expression of dynamin mutants that lack GTPase activity, have impaired self-assembly, or exhibit compromised membrane binding can inhibit native dynamin function, causing a dominant-negative effect on transferrin uptake since dynamin functions depend on self-assembly of soluble subunits (predominantly tetramers, few dimers) in an optimally functional polymer^{137,138}. Therefore, this experimental approach is relevant for understanding potential mutations linked to Charcot-Marie-Tooth neuropathy, as these mutations typically follow an autosomal dominant pattern.

To test dynamin1 functions specifically, we used dynamin2 knock-out HeLa cells, which have been reported before³⁹. The predominantly expressed dynamin paralog in HeLa cells is dynamin2. Upon dynamin2 knock-out, these cells survive due to compensation of essential dynamin2 functions by dynamin1 expressed in lower levels in these cells, albeit with pronounced growth defects. To evaluate functions of VL4 mutants in cells, we employed a well-established cellular assay to assess dynamin's role in clathrin-mediated endocytosis. As a read-out for dynamin functions, we monitored the internalization of canonical clathrin-dependent cargo, transferrin. For these experiments, dynamin1 mutants in the VL4 region were overexpressed in Dyn2^{KO} HeLa cells. Notably, these cells showed dramatically lower levels of transferrin uptake in comparison to the wild type HeLa, a testament to the fact that these cells in fact express only low levels of dynamin1, merely sufficient for survival.

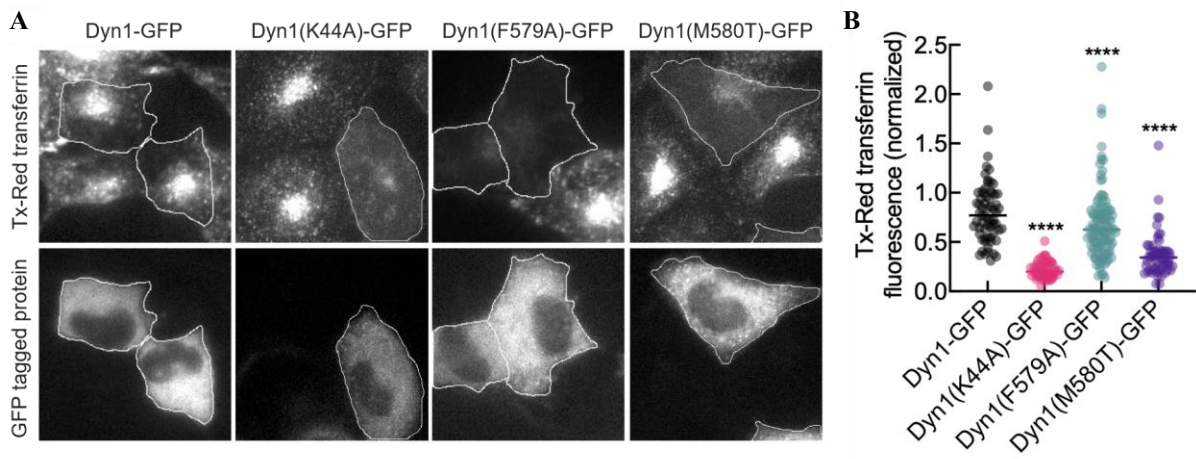


Figure 8.1 Assaying cellular functions of dynamin by estimating transferrin-uptake.

A. Representative micrographs showing intensity of internalised transferrin in Dyn2^{KO} HeLa cells to specifically test Dyn1 functions. For these assays, the cells were fed with excess TexasRed-transferrin for 10 minutes at 37 °C, then washed off to remove unbound ligand and imaged to visualise internalised transferrin. Overexpression of VL4 mutants of Dyn1 causes defects in uptake of transferrin, as seen in transfected cells (GFP positive cells seen in the bottom panel). Top panel shows punctate fluorescence of internalised transferrin in non-transfected as well as transfected cells (white outline indicates cell boundaries) expressing Dyn1-GFP and VL4 mutants of Dyn1 tagged to GFP. **B.** Quantification of data in A. Total number of cells sampled (n) in at least two independent experiments for each Dyn1 construct are indicated as follows: Dyn1-GFP (n = 84), Dyn1(K44A)-GFP (n = 57), Dyn1(F579A)-GFP (n = 109), and Dyn1(M580T)-GFP (n = 58). Data were normalized to the mean transferrin fluorescence seen in non-transfected cells for each case. Significance was estimated using Mann-Whitney's test where **** denotes P < 0.0001.

As a negative control, cells with overexpression of the GTPase-defective mutant Dyn1(K44A)-GFP⁸⁴ showed little to no transferrin uptake thus exhibiting almost completely disrupted CME compared to cells expressing Dyn1-GFP (Figure 8.1). Notably, mutants with reduced hydrophobicity in VL4 also exhibited severe defects in cellular functions. Overexpression of Dyn1(F579A)-GFP and the CMT-linked mutant Dyn1(M580T)-GFP resulted in a significant reduction in transferrin uptake. This reduction is evident from the loss of intense perinuclear transferrin fluorescence observed in cells expressing the mutant proteins compared to non-transfected cells and a quantifiable decrease in overall transferrin fluorescence associated with these cells. However, very low levels of internalized transferrin in some cells were apparent, slightly above the internalized transferrin fluorescence observed in cells expressing Dyn1(K44A)-GFP. This was still dramatically lower than the levels of

transferrin internalized by Dyn1-GFP expressing cells emphasizing the critical nature of VL4 functions for efficient vesicle release by dynamin during clathrin-mediated endocytosis.

8.3 Discussion

Clathrin-mediated endocytosis is one of the most widely studied and best understood cellular phenomenon. Since dynamin functions during clathrin-mediated endocytosis proceed by virtue of its higher order oligomer forming properties, endogenously and exogenously expressed forms of dynamin could co-polymerize in cells, allowing the deleterious effects of exogenously expressed mutants to become apparent as dominant negative effects in dynamin function. Hence, we exploited a widely-used assay well established in literature to examine how reducing the hydrophobic character of VL4 impacts dynamin functions. Our results upon expressing Dyn1 mutants in Dyn2^{KO} cells unambiguously and quantitatively show that Dyn1 F579A and Dyn1 M580T both have detrimental effects on clathrin-mediated endocytosis. These findings align with the results from in vitro assays that indicate a defect in membrane fission, suggesting a critical role for VL4 in dynamin functions.

Remarkably, a gradation of disruption of CME is apparent from quantitation of internalised transferrin in transfected cells. Dyn1 K44A, the GTP-hydrolysis mutant nearly shuts down CME. Dyn1 F579A, the more subtle mutation perturbing VL4 hydrophobic character only slightly, shows an intermediate effect on CME, somewhere between the Dyn1 and Dyn1 K44A expression phenotypes. Dyn1 M580T, the disease-linked mutant with VL4 hydrophobic character majorly perturbed, shows significantly more disruption in CME than Dyn1 F579A, with the phenotype being closer to that seen in case of Dyn1 K44A. Yet, Dyn1 M580T did not completely abrogate CME.

It's worth noting that the impact overexpression of the VL4 mutants on CME was not as severe as that observed with overexpression of Dyn1(K44A), which may explain why the CMT-linked mutation is debilitating but not lethal. Arguably, if such mutations were indeed lethal, they would not be identified in adults anyhow.

Chapter 9

SUMMARY, DISCUSSION AND PERSPECTIVES

Summary: Our findings in brief

To corroborate experimental evidence for the recent findings from molecular dynamics (MD) simulations¹⁰³ and structural modeling^{52,94} that revealed that a novel variable loop 4 or VL4 in the dynamin PH-domain forms a membrane-inserting anchor, and together with the previously known VL1 plays a role in stabilizing dynamin PHD on the membrane, we performed fine biochemical and cellular analysis. Although the importance of VL1 membrane insertion has been previously established¹⁰², our study is the first to experimentally investigate the significance of VL4 membrane insertion in dynamin's functions. In this study, we tested dynamin mutants in the VL4 tip region that perturb the hydrophobic or the electrostatic nature of the loop, in conditions that progressively and closely mimic physiological context of dynamin function.

Dyn F579A that exhibits a subtle mutation slightly reducing hydrophobicity at the tip of VL4, was seen to have lower membrane binding affinity or K_d . Results from these bulk liposomes binding assays also showed that VL4 is an additional membrane binding site in the dynamin PHD, over the previously known VL1, as Dyn1 F579A showed a marked decrease in the B_{max} achieved by the protein.

Complementing these assays and analysing the membrane binding reaction more closely, we performed microscopic assays with Dyn1 F579A and Dyn1 M580T, the VL4 mutant associated with the pathology of the congenital Charcot-Marie-Tooth neuropathy which perturbs VL4 hydrophobic character much more than the subtler F579A mutation, on supported membrane nanotubes to assess their membrane binding capacities. Expanding our analysis to membrane nanotubes of different dimensions presented with added advantage of probing the role membrane curvature in these functions as curved membranes display more membrane defects, which is known to form binding sites for hydrophobic moieties. We investigated the role of VL4 in membrane binding and observed that Dyn1 F579A as well as M580T formed few to no foci of dynamin scaffolds on membrane nanotubes. Since this setup involved washing-off of excess unbound protein, we found that VL4 mutants loosely and not stably bind membrane nanotubes of narrow dimensions. Across a range of diameters in which dynamin1 shows a rather shallow curvature preference for membrane binding, VL4 mutants showed a steep decline displaying a much more curvature-sensitive membrane binding activity. In presence of nucleotide and co-factors, these mutants showed partial fission activity in a tube-size dependent manner. We argued that curved membrane surfaces expose more defects in the membrane thereby facilitating binding of hydrophobic patches. Notably, Dyn1 K583A that

perturbs the basic character of the loop did not show any defects in membrane fission under similar conditions. Importantly, Dynamin2, inherently being more sensitive to membrane curvature displayed complete abrogation in both membrane-binding and fission upon introduction of VL4 mutations that lead to reduced hydrophobicity. While VL4 mutants showed a steeper curvature-sensitivity, arguably because membrane defects allosterically stabilise dynamin on membrane by exposing more binding pockets for hydrophobic patches in the protein. They also showed only partial binding and fission propensity even in the narrow range of tube radii, pointing to additional defects. Membrane binding and oligomerisation are tightly coupled for endocytic dynamins because of the underlying PH-domain (C-terminal helix) and stalk interactions that maintains dynamin in an auto-inhibited state in solution. This auto-inhibition is released when PHD engages with the membrane, therefore facilitating rapid oligomerisation of dynamin on membranes. In case of unstable or loose peripheral binding of PHD to the membrane which is the case with VL4 mutants, the downstream steps i.e., oligomerisation, stimulated GTPase activity and in-turn membrane fission would intuitively be affected. Thus, in this case, where stable dynamin recruitment and polymerisation solely depends on its lipid-binding, it is difficult to analyse whether VL4-membrane insertion physically facilitates the membrane fission process beyond the regime of stabilising membrane anchorage.

Importantly, comparative analysis of the effect of VL1 and VL4 insertion on dynamin function revealed opposite and discrete effects of variable loops on dynamin-mediated membrane fission, in light of key literature and recent findings from *in-silico* and experimental studies. Our results emphasized that variable loop insertion can lead to opposite effects on dynamin fission. In this context, VL1 insertion facilitates constriction of the membrane whereas VL4 insertion facilitates membrane fission. The underlying reason for these distinct effects on dynamin function is not clear but it is probable that either regulated or stochastic insertion of either or both loops in dynamin subunits in a scaffold leads to a finely orchestrated outcome of membrane fission, also highlighting that membrane fission by dynamin is in fact a highly regulated process.

In order to test whether VL4 membrane insertion has a physical role in promoting dynamin-mediated membrane fission, we utilized a more native-like setup for recruiting dynamin to the membrane and then specifically testing its membrane fission activity. In our fluorescence-based supported membrane nanotube assays, we first recruited a dynamin binding partner or adaptor protein BIN1, a BAR domain-containing protein that engages with dynamin PRD via

its SH3 domains. BIN1 readily bound 1 mole percent PIP₂ containing nanotubes and formed scaffolds constricting the underlying tube to narrower dimensions. BIN1 induced membrane constriction has been reported here for the first time, although BIN1-induced membrane tubulation has previously been documented. BIN1 scaffolds constricted the underlying tube but conformed to the initial tube radius to some extent suggesting flexible and plastic scaffolding activity. BIN1-induced membrane constriction showed only a shallow dependence on starting tube radius, however, these represented SH3-dense regions that had tube dimensions well within the range in which Dyn1 F579A showed partial fission activity. These scaffolds readily recruited Dyn1 F579A, as seen by the tightly correlated discrete foci of both proteins. To extreme surprise however, in presence of GTP and co-factors, while Dyn1 showed robust fission that led to membrane severing right in the middle of an underlying BIN1 scaffold, Dyn1 F579A completely failed in membrane fission. So, instead of rescuing Dyn1 F579A functions on tubes that efficiently recruit it in a native-like manner, as well as sport favourable dimensions for fission, these experiments instead highlighted a different very important aspect of this process i.e., subtle changes in membrane affinity can lead to exaggeration of observed defects in presence of binding partners that compete for the same lipids in the membrane.

Following this, we further investigated Dyn1 F579A and M580T functions in cellular assays by analysing uptake of fluorescently labelled canonical CME cargo, transferrin. In HeLa cells that have dynamin2, the predominant form of dynamin knocked out, we tested specifically for dynamin1 functions. Expression of Dyn1 K44A that is a hydrolysis mutant of Dyn1 has a dominant negative effect on the endogenous Dyn1 functions in these cells which inherently express only low levels of Dyn1. Dyn1 K44A expression showed no transferrin uptake in these cells and acted as a negative control. Expression of both Dyn1 F579A and M580T showed a dramatic defect in transferrin internalisation.

In summary, our results establish an indispensable role for VL4-membrane engagement in dynamin-mediated membrane fission. Importantly, our mechanistic analysis reveals a detailed molecular picture of underlying defects associated with the autosomal dominant form of CMT-neuropathy linked phenotypes arising from a pathological mutation M580T in VL4 region of dynamin2. This work also highlights that it is vital to design tools and assays that allow closely mimicking these native-like conditions in order to gain valuable insights on physiological functions of membrane-active proteins.

Discussion: Our findings in the context of literature

Results from MD simulations largely align with structural modeling of the PHD within a cryo-EM map of membrane-bound dynamin1 polymer, although differences may be attributed to variations in membrane composition, curvature and limited resolution in the cryo-EM map, demonstrating that VL4 serves as the second preferred anchor for membrane insertion, following VL1, and together, these loops contribute to the stabilization of dynamin on the membrane^{83,103,94,52}. The importance of VL4 in dynamin's membrane binding and fission processes becomes apparent on membranes displaying physiologically relevant lipid compositions. Mutations reducing VL4's hydrophobicity have adverse effects on membrane binding in liposome-based bulk assays with physiological PIP₂ levels which highlight slight defects in membrane binding attributes of VL4 mutants such as K_d and B_{max} .

Dynamin possesses the capability to self-assemble into helical scaffolds, and its binding is inherently favoured on membranes with high curvature due to exposed membrane defects that facilitate binding of hydrophobic moieties¹³⁹. However, dynamin scaffolds have the unique ability to constrict membranes, thereby expanding the range of curvatures that can support binding and self-assembly. A key role for VL4 in dynamin-induced membrane curvature becomes apparent upon sampling supported membrane nanotubes of varying dimensions, as Dyn1 VL4 mutants shows a sharp reduction in binding as membrane curvature decreases. Nonetheless, on tubes within a size range where the VL4 mutants still bind even partially, their addition with GTP induces fission in case of Dyn1, indicating that these mutants exhibit partial functional defects. In other words, we discover that VL4 mutants make Dyn1 and Dyn2 functions more curvature-sensitive. As a result, dynamin1 mutants show partial activity on thinner tubes whereas dynamin2 mutants are practically dead in membrane-fission, since Dyn2 functions inherently have more dependence on membrane curvature. Importantly, detrimental effects associated with mutants that reduce VL4 hydrophobicity, but not charge, are observed in our assays. However, VL4 mutants can still induce fission on tubes accommodating their size range, showing partial functional defects.

Earlier experiments where Dyn1 Δ PHD^{6xHis} was recruited to the membrane using chelating lipids and yet it showed membrane fission have indicated a catalytic contribution of the PHD in dynamin-mediated membrane fission¹¹¹. However, in the aforementioned, fission occurred at a markedly slower rate such that each fission event proceeded with a long-lived highly constricted tubular intermediate. This phenomenon can be attributed to the observation that the insertion of variable loops induces non-bilayer-like arrangements of membrane lipids, reducing

the energy required for membrane bending^{127,103}. Our recently published findings extend beyond these established models and unveil that variable loops have distinct and separable effects on dynamin functions. VLS also display a certain level of exclusivity in their membrane engagement, perhaps due to restrictive mobility arising from steric factors when confined in a polymer^{52,94}. This exclusivity is stark as that is what enabled us to categorize the modelled PHDs into distinct clusters based on which VL is inserted into the membrane. This observation suggests negative allostery, where the insertion of one VL hinders the insertion of another VL through an as-yet-unknown relay mechanism.

This selectivity is further demonstrated in how VLS influence dynamin's ability to constrict membranes and promote membrane fission. There is a growing body of evidence supporting a model in which the pleckstrin homology domain, through its variable loops, actively influences the fission reaction but the underlying mechanism is obscure. Molecular dynamics simulations of the PHD show that the F579A mutation causes VL1 to insert more deeply into the membrane, while the I533A mutation has no effect on VL4. The requirement for a greater degree of constriction for fission with the VL4 mutant may arise from the deeper insertion of VL1. In our assays, a comparative analysis of VL1 and VL4 mutants shows that VL1 facilitates dynamin-induced constriction, whereas VL4 restrains the dynamin scaffold from constricting tubes, rather promotes fission. Furthermore, fission with dynamin occurs when tubes constrict to a pre-fission intermediate with a radius of approximately 5 nm. However, with the VL1 mutant, fission occurs at a wider intermediate radius of around 6.4 nm, suggesting that VL1 negatively affects the fission process. In contrast, fission with the VL4 mutant is achieved when tubes constrict to a thinner intermediate radius of approximately 3.4 nm, indicating that VL4 promotes fission. These results together uncover the molecular details underlying the catalytic functions of PH-domain in dynamin-mediated membrane fission that we have alluded to in our previous studies^{52,111}.

Endocytic dynamins rely on a combination of complex interactions involving both proteins and lipids to perform their essential functions within the cell. Protein-protein interactions play a crucial role in recruiting dynamins to specific cellular locations, while protein-lipid interactions are key determinants for the fission process. Therefore, we hypothesized that dual-mode recruitment of dynamin to membrane templates mediated by both protein and lipid interactions could compensate for the partial lipid-binding defects in Dyn1 F579A and ensure rescue of Dyn1 F579A functions in membrane fission. BIN1, a BAR domain-containing protein and dynamin binding partner formed scaffolds exhibiting discrete foci on a particular

range of membrane nanotubes, displaying high local concentration of SH3 domains, and was found to have the capability to constrict membrane tubes to a size suitable for fission by Dyn1 F579A. Importantly, the experimental setup ruled out the formation of mixed scaffolds that have been linked with inhibition in dynamin function, by ensuring sequential recruitment of the two proteins with an additional step to wash-off excess unbound BIN1 from the reaction chamber. Surprisingly, despite Dyn1 F579A effectively binding to BIN1 scaffolds, it completely failed to induce fission unlike Dyn1 WT. Arguably, BIN1 scaffolds facilitate dynamin recruitment to the membrane despite Dyn1 F579A's lipid-binding defects, but they may compete with dynamin for PIP₂ binding. We attribute the failure for Dyn1 F579A to show fission to limiting PIP₂ levels in the membrane, due to which with even slightly reduced affinity of Dyn1 F579A for PIP₂ dramatically impacts its ability to engage with the membrane in the presence of the competitive binding partners such as BIN1.

Consequently, this study sheds light on a general cellular phenomenon, that is, endocytic partner proteins can act in a mutually competitive manner. While partner protein interactions facilitate the recruitment of dynamin, these very partners may also compete for binding to the same lipids, which could prove to be limiting thereby dynamin's engagement with the membrane. As a result, even subtle defects in membrane binding can become amplified within the localized microenvironment of the BIN1 scaffold, rendering the VL4 mutant absolutely ineffective in mediating fission of the underlying membrane tube and clathrin-mediated endocytosis.

The PHD represents a focal point for genetic mutations responsible for various genetic disorders. A significant portion of these mutations is located within regions that exhibit a high degree of conservation across all dynamin isoforms. Our research builds upon these findings by delving into the functions of VL4 within dynamin. Expression of Dyn1 F579A and Dyn1 M580T in cells lead to disruption of clathrin-mediated endocytosis. Therefore, we conclude that VL4-membrane insertion by virtue of its hydrophobic character is absolutely critical for facilitating dynamin mediated membrane fission.

Finally, as a broader principle in cell biology, our findings underscore the finely tuned evolution of lipid-protein interactions, which play a crucial role in facilitating efficient vesicle release by dynamin-mediated membrane fission during clathrin-mediated endocytosis. The evidence from our biochemical and cellular assays put together, provides a mechanistic basis for understanding the fundamental role of PH-domain in dynamin function, and in-turn for developing therapeutic aids for associated disorders.

Perspectives, and things to wonder!

Intriguingly, the PH-domain is actually a recurring feature in many intracellular signaling proteins in the human proteome⁹⁰⁻⁹². PHD exhibits a modest affinity for phosphoinositides or phosphatidylinositol lipids¹⁰⁰. Like dynamins, the PH-domain imparts lipid-binding characteristics to various proteins consisting this module, albeit, they are known to perform very diverse functions in the cell. Some examples of such PH-domain-containing proteins are Pleckstrin, Spectrin, and Phospholipase-C δ or PLC δ ⁹⁷. PHDs of different proteins can distinguish distinct phosphoinositides by recognizing the geometry of phosphates on the inositol head group⁹⁶. This characteristic trait equips proteins containing a *pleckstrin homology domain* with the ability to bind to particular intracellular membranes enriched with specific phosphatidylinositol lipids, thereby contributing to organelle identification and specific downstream signalling^{100,140}.

The authors who reported the PH-domain crystal structure for the first time called the variable loops so due to their varying sequence among PHDs of different proteins and reasoned that this variation is akin to the variable region of antibodies⁹³. We now have sufficient evidence in literature that suggests that in fact, variable loops have a function very similar to that of the variable regions of antibodies. As in, while the immunoglobulin variable chains confer specificity to different antigens, the VLs have perhaps evolved in a divergent manner in different proteins as the modular ends of the protein, conferring them with specificity to different phosphoinositides and therefore directing them towards very diverse functions in the cell. The PH-fold can therefore be thought of as a scaffold on which unstructured loops with highly disparate sequences are presented that impart functionality.

Remarkably, at present, there are 269 reviewed entries of proteins with a PHD in the human genome, yet very little is known about the number and function of different variable loops in these proteins. Additionally, variable loop membrane insertion could be a common feature of other PHDs and significantly impact protein functions. However, it remains completely unexplored whether these VLs insert into membranes and have underlying common or unique functional features associated with each of these proteins. Analysing the structural homology between these PHDs and the dynamin PHD could offer valuable insights, making it an exciting area for future research.

Publications and permissions

Research articles

1. **Khurana H.**, Baratam K., Bhattacharyya S., Srivastava A., Pucadyil T.J. 2023. Mechanistic analysis of a novel membrane interacting variable loop in the pleckstrin-homology domain critical for dynamin function. **PNAS** (doi: 10.1073/pnas.2215250120)

Note: Parts of this research article were included in the presented thesis. Relevant permissions are stated below and can be found at [/pnas.org/about/rights-permissions](https://pnas.org/about/rights-permissions).

PNAS

RESEARCH ARTICLE

BIOCHEMISTRY



Mechanistic analysis of a novel membrane-interacting variable loop in the pleckstrin-homology domain critical for dynamin function

Himani Khurana[#] , Krishnakanth Baratam[°] , Soumya Bhattacharyya[#] , Anand Srivastava[°] , and Thomas J. Pucadyil^{#,1}

Edited by James Hurley, University of California Berkeley, Berkeley, CA; received September 6, 2022; accepted February 8, 2023

PNAS

ARTICLES ▾ FRONT MATTER AUTHORS ▾ TOPICS +



SIGN IN

SUBMIT

PNAS authors do not need to obtain permission in the following cases:

1. to use their original figures or tables in their future works;
2. to make copies of their articles for their own personal use, including classroom use, or for the personal use of colleagues, provided those copies are not for sale and are not distributed in a systematic way;
3. to include their articles as part of their dissertations; or
4. to use all or part of their articles in printed compilations of their own works.

The full journal reference must be cited and, for articles published in volumes 90–105 (1993–2008), "Copyright (copyright year) National Academy of Sciences" must be included as a copyright note.

2. Andhare D.S.[#], **Khurana H.**[#], Pucadyil T.J. 2022. ([#]co-first authorship) Protein-protein interactions on membrane surfaces analysed using pull downs with supported bilayers on silica beads. **Journal of Membrane Biology** (doi: 10.1007/s00232-022-00222-4)

Review articles

1. **Khurana H.** and Pucadyil T.J. 2023. 'Gearing' up for dynamin-catalyzed membrane fission. **Current Opinion in Cell Biology** (doi: 10.1016/j.ceb.2023.102204)

In progress

1. Yogita Kapoor, **Himani Khurana**, Arnab Chakraborty, Nitesh Kumar Singh, Anshu Priya, Archana Singh, Divya Tej Sowpati, Siddhesh Kamat, Thomas J. Pucadyil, Vinay Kumar Nandicoori. Wag31, a membrane tether, is crucial for cellular homeostasis in Mycobacterium. (Submitted, presently under editorial review)
2. Vani Pande, **Himani Khurana**, Thomas J. Pucadyil, Gayathri Pananghat. Analysis of nucleotide-dependent membrane remodeling activity of bacterial cell shape determining actin-homolog MreB. (Manuscript in preparation)

References

1. Leonard TA, Loose M, Martens S. The membrane surface as a platform that organizes cellular and biochemical processes. *Developmental Cell*. Published online July 6, 2023. doi:10.1016/j.devcel.2023.06.001
2. Posor Y, Jang W, Haucke V. Phosphoinositides as membrane organizers. *Nat Rev Mol Cell Biol*. 2022;23(12):797-816. doi:10.1038/s41580-022-00490-x
3. Vance JE. Phospholipid Synthesis and Transport in Mammalian Cells. *Traffic*. 2015;16(1):1-18. doi:10.1111/tra.12230
4. Porter KR, Claude A, Fullam EF. A STUDY OF TISSUE CULTURE CELLS BY ELECTRON MICROSCOPY. *Journal of Experimental Medicine*. 1945;81(3):233-246. doi:10.1084/jem.81.3.233
5. Li D, Shao L, Chen BC, et al. ADVANCED IMAGING. Extended-resolution structured illumination imaging of endocytic and cytoskeletal dynamics. *Science*. 2015;349(6251):aab3500. doi:10.1126/science.aab3500
6. Valm AM, Cohen S, Legant WR, et al. Applying systems-level spectral imaging and analysis to reveal the organelle interactome. *Nature*. 2017;546(7656):162-167. doi:10.1038/nature22369
7. Heinrich L, Bennett D, Ackerman D, et al. Whole-cell organelle segmentation in volume electron microscopy. *Nature*. 2021;599(7883):141-146. doi:10.1038/s41586-021-03977-3
8. Palade G. Intracellular Aspects of the Process of Protein Synthesis. *Science*. 1975;189(4200):347-358. doi:10.1126/science.1096303
9. Novick P, Ferro S, Schekman R. *Order of Events in the Yeast Secretory Pathway*. Vol 25.; 1981:461-469.
10. Mellman I, Warren G. The road taken: past and future foundations of membrane traffic. *Cell*. 2000;100(1):99-112. doi:10.1016/s0092-8674(00)81687-6
11. Bonifacino JS, Glick BS. The Mechanisms of Vesicle Budding and Fusion. *Cell*. 2004;116(2):153-166. doi:10.1016/S0092-8674(03)01079-1
12. Rothman JE. The protein machinery of vesicle budding and fusion. *Protein Science*. 2008;5(2):185-194. doi:10.1002/pro.5560050201
13. Schekman R. Charting the Secretory Pathway in a Simple Eukaryote. *Molecular Biology of the Cell*. 2010;21(22):3781-3784. doi:10.1091/mbc.e10-05-0416
14. Mellman I, Emr SD. A Nobel Prize for membrane traffic: Vesicles find their journey's end. *The Rockefeller University Press J Cell Biol*. 2013;203:559-561. doi:10.1083/jcb.201310134
15. Bonifacino JS. Vesicular transport earns a Nobel. *Trends in Cell Biology*. 2014;24(1):3-5. doi:10.1016/j.tcb.2013.11.001

16. Schekman R. *Genes and Proteins That Control the Secretory Pathway*. Vol 209.; 2015:35-61. doi:10.1051/jbio/2015011
17. Spang A. Anniversary of the discovery of sec mutants by Novick and Schekman. *Molecular Biology of the Cell*. 2015;26(10):1783-1785. doi:10.1091/mbc.e14-11-1511
18. Antonny B. Membrane deformation by protein coats. *Current Opinion in Cell Biology*. 2006;18(4):386-394. doi:10.1016/j.ceb.2006.06.003
19. Stagg SM, LaPointe P, Balch WE. Structural design of cage and coat scaffolds that direct membrane traffic. *Curr Opin Struct Biol*. 2007;17(2):221-228. doi:10.1016/j.sbi.2007.03.010
20. Spang A. The life cycle of a transport vesicle. *Cell Mol Life Sci*. 2008;65(18):2781-2789. doi:10.1007/s00018-008-8349-y
21. Faini M, Beck R, Wieland FT, Briggs JAG. Vesicle coats: structure, function, and general principles of assembly. *Trends Cell Biol*. 2013;23(6):279-288. doi:10.1016/j.tcb.2013.01.005
22. Conner SD, Schmid SL. Regulated portals of entry into the cell. *Nature*. 2003;422(6927):37-44. doi:10.1038/nature01451
23. Schmid SL, Sorkin A, Zerial M, Lewis WH. Endocytosis : Past , Present , and Future. 2014;3:1-9.
24. Schmid SL. CLATHRIN-COATED VESICLE FORMATION AND PROTEIN SORTING: An Integrated Process. *Annual Review of Biochemistry*. 1997;66(1):511-548. doi:10.1146/annurev.biochem.66.1.511
25. Robinson MS. Adaptable adaptors for coated vesicles. *Trends Cell Biol*. 2004;14(4):167-174. doi:10.1016/j.tcb.2004.02.002
26. Haucke V, Kozlov MM. Membrane remodeling in clathrin-mediated endocytosis. *Journal of Cell Science*. 2018;131(17):jcs216812. doi:10.1242/jcs.216812
27. Kaksonen M, Toret CP, Drubin DG. A modular design for the clathrin- and actin-mediated endocytosis machinery. *Cell*. 2005;123.
28. Rappoport JZ. Focusing on clathrin-mediated endocytosis. *Biochem J*. 2008;412.
29. Mettlen M, Loerke D, Yarar D, Danuser G, Schmid SL. Cargo- and adaptor-specific mechanisms regulate clathrin-mediated endocytosis. *J Cell Biol*. 2010;188.
30. Traub LM. Regarding the amazing choreography of clathrin coats. *PLoS Biology*. 2011;9(3). doi:10.1371/JOURNAL.PBIO.1001037
31. McMahon HT, Boucrot E. Molecular mechanism and physiological functions of clathrin-mediated endocytosis. *Nature Reviews Molecular Cell Biology*. 2011;12(8):517-533. doi:10.1038/nrm3151

32. Kirchhausen T, Owen D, Harrison SC. Molecular structure, function, and dynamics of clathrin-mediated membrane traffic. *Cold Spring Harbor Perspectives in Biology*. 2014;6(5). doi:10.1101/cshperspect.a016725
33. Kaksonen M, Roux A. Mechanisms of clathrin-mediated endocytosis. *Nature Reviews Molecular Cell Biology*. 2018;19(5):313-326. doi:10.1038/nrm.2017.132
34. Heymann JAW, Hinshaw JE. Dynamins at a glance. *Journal of Cell Science*. 2009;122:3427-3431. doi:10.1242/jcs.051714
35. Praefcke GJK, McMahon HT. The dynamin superfamily: Universal membrane tubulation and fission molecules? *Nature Reviews Molecular Cell Biology*. 2004;5(2):133-147. doi:10.1038/nrm1313
36. Daumke O, Praefcke GJK. Invited review: Mechanisms of GTP hydrolysis and conformational transitions in the dynamin superfamily. *Biopolymers*. 2016;105(8):580-593. doi:10.1002/bip.22855
37. Jimah JR, Hinshaw JE. Structural Insights into the Mechanism of Dynamin Superfamily Proteins. *Trends in Cell Biology*. 2019;29(3):257-273. doi:10.1016/j.tcb.2018.11.003
38. Ramachandran R, Schmid SL. The dynamin superfamily. *Current Biology*. 2018;28(8):R411-R416. doi:10.1016/j.cub.2017.12.013
39. Kamerkar SC, Kraus F, Sharpe AJ, Pucadyil TJ, Ryan MT. Dynamin-related protein 1 has membrane constricting and severing abilities sufficient for mitochondrial and peroxisomal fission. *Nature Communications*. 2018;9(1):1-15. doi:10.1038/s41467-018-07543-w
40. Ford MGJ, Chappie JS. The structural biology of the dynamin-related proteins: New insights into a diverse, multitasking family. *Traffic*. 2019;20(10):717-740. doi:10.1111/tra.12676
41. Kraus F, Roy K, Pucadyil TJ, Ryan MT. Function and regulation of the divisome for mitochondrial fission. *Nature*. 2021;590(7844):57-66. doi:10.1038/s41586-021-03214-x
42. Hu J, Rapoport TA. Fusion of the endoplasmic reticulum by membrane-bound GTPases. *Semin Cell Dev Biol*. 2016;60:105-111. doi:10.1016/j.semcdb.2016.06.001
43. Gao S, Hu J. Mitochondrial Fusion: The Machineries In and Out. *Trends in Cell Biology*. 2021;31(1):62-74. doi:10.1016/j.tcb.2020.09.008
44. Naslavsky N, Caplan S. EHD proteins: key conductors of endocytic transport. *Trends Cell Biol*. 2011;21(2):122-131. doi:10.1016/j.tcb.2010.10.003
45. Bhattacharyya S, Pucadyil TJ. Cellular functions and intrinsic attributes of the ATP-binding Eps15 homology domain-containing proteins. *Protein Science*. 2020;29(6):1321-1330. doi:10.1002/pro.3860
46. Haller O, Staeheli P, Schwemmle M, Kochs G. Mx GTPases: dynamin-like antiviral machines of innate immunity. *Trends Microbiol*. 2015;23(3):154-163. doi:10.1016/j.tim.2014.12.003

47. Schmid SL, Frolov VA. Dynamin: Functional Design of a Membrane Fission Catalyst. *Annual Review of Cell and Developmental Biology*. 2011;27(1):79-105. doi:10.1146/annurev-cellbio-100109-104016
48. Faelber K, Held M, Gao S, et al. Structural insights into dynamin-mediated membrane fission. *Structure*. 2012;20(10):1621-1628. doi:10.1016/j.str.2012.08.028
49. Ferguson SM, De Camilli P. Dynamin, a membrane-remodelling GTPase. *Nature reviews Molecular cell biology*. 2012;13(2):75-88. doi:10.1038/nrm3266
50. Chappie JS, Dyda F. Building a fission machine - structural insights into dynamin assembly and activation. *Journal of Cell Science*. 2013;126:2773-2784. doi:10.1242/jcs.108845
51. Antony B, Burd C, De Camilli P, et al. Membrane fission by dynamin: what we know and what we need to know. *The EMBO Journal*. 2016;35(21):2270-2284. doi:10.15252/embj.201694613
52. Khurana H, Pucadyil TJ. "Gearing" up for dynamin-catalyzed membrane fission. *Current Opinion in Cell Biology*. 2023;83:102204. doi:10.1016/j.ceb.2023.102204
53. Ford MGJ, Jenni S, Nunnari J. The crystal structure of dynamin. *Nature*. 2011;477(7366):561-566. doi:10.1038/nature10441
54. Faelber K, Posor Y, Gao S, et al. Crystal structure of nucleotide-free dynamin. *Nature*. 2011;477(7366):556-562. doi:10.1038/nature10369
55. Reubold TF, Faelber K, Plattner N, et al. Crystal structure of the dynamin tetramer. *Nature*. 2015;525(7569):404-408. doi:10.1038/nature14880
56. Mettlen M, Pucadyil T, Ramachandran R, Schmid SL. Dissecting dynamin's role in clathrin-mediated endocytosis. *Biochemical Society transactions*. 2009;37(Pt 5):1022. doi:10.1042/BST0371022
57. Daumke O, Roux A, Haucke V. BAR domain scaffolds in dynamin-mediated membrane fission. *Cell*. 2014;156(5):882-892. doi:10.1016/j.cell.2014.02.017
58. Cocucci E, Gaudin R, Kirchhausen T. Dynamin recruitment and membrane scission at the neck of a clathrin-coated pit. *Molecular Biology of the Cell*. 2014;25(22):3595-3609. doi:10.1091/mbc.e14-07-1240
59. Nakata T, Iwamoto A, Noda Y, Takemura R, Yoshikura H, Hirokawa N. Predominant and developmentally regulated expression of dynamin in neurons. *Neuron*. 1991;7(3):461-469. doi:10.1016/0896-6273(91)90298-E
60. Cao H, Garcia F, McNiven MA. Differential Distribution of Dynamin Isoforms in Mammalian Cells. *Molecular Biology of the Cell*. 1998;9(9):2595-2609. doi:10.1091/mbc.9.9.2595
61. Sontag JM, Fykse EM, Ushkaryov Y, Liu JP, Robinson PJ, Südhof TC. *Differential Expression and Regulation of Multiple Dynamins*. Vol 269.; 1994:4547-4554.

62. Gray NW, Kruchten AE, Chen J, McNiven MA. A dynamin-3 spliced variant modulates the actin/cortactin-dependent morphogenesis of dendritic spines. *J Cell Sci.* 2005;118(Pt 6):1279-1290. doi:10.1242/jcs.01711
63. Vaid KS, Guttman JA, Babyak N, et al. The Role of Dynamin 3 in the Testis. *Journal of cellular physiology.* 2007;207(1):581-588. doi:10.1002/JCP
64. Cook TA, Urrutia R, McNiven MA. Identification of dynamin 2, an isoform ubiquitously expressed in rat tissues. *Molecular and Cellular Biology.* 2010;30(3):781-792. doi:10.1128/mcb.00330-09
65. Fan F, Funk L, Lou X. Dynamin 1- and 3-Mediated Endocytosis Is Essential for the Development of a Large Central Synapse In Vivo. *J Neurosci.* 2016;36(22):6097-6115. doi:10.1523/JNEUROSCI.3804-15.2016
66. Shi B, Jin YH, Wu LG. Dynamin 1 controls vesicle size and endocytosis at hippocampal synapses. *Cell Calcium.* 2022;103:102564. doi:10.1016/j.ceca.2022.102564
67. Liu YW, Neumann S, Ramachandran R, Ferguson SM, Pucadyil TJ, Schmid SL. Differential curvature sensing and generating activities of dynamin isoforms provide opportunities for tissue-specific regulation. Published online 2011. doi:10.1073/pnas.1102710108
68. Ferguson S, Raimondi A, Paradise S, et al. Coordinated Actions of Actin and BAR Proteins Upstream of Dynamin at Endocytic Clathrin-Coated Pits. *Developmental Cell.* 2009;17(6):811-822. doi:10.1016/j.devcel.2009.11.005
69. Park RJ, Shen H, Liu L, Liu X, Ferguson SM, De Camilli P. Dynamin triple knockout cells reveal off target effects of commonly used dynamin inhibitors. *Journal of Cell Science.* 2013;126(22):5305-5312. doi:10.1242/jcs.138578
70. Bhave M, Mettlen M, Wang X, Schmid SL. Early and non-redundant functions of dynamin isoforms in clathrin-mediated endocytosis. *Molecular Biology of the Cell.* Published online 2020:mbc.E20-06-0363. doi:10.1091/mbc.e20-06-0363
71. Raimondi A, Ferguson SM, Lou X, et al. Overlapping Role of Dynamin Isoforms in Synaptic Vesicle Endocytosis. *Neuron.* 2011;70(6):1100-1114. doi:10.1016/j.neuron.2011.04.031
72. Gómez-Oca R, Edelweiss E, Djeddi S, et al. Differential impact of ubiquitous and muscle dynamin 2 isoforms in muscle physiology and centronuclear myopathy. *Nat Commun.* 2022;13(1):6849. doi:10.1038/s41467-022-34490-4
73. Laiman J, Hsu YJ, Loh J, et al. GSK3 α phosphorylates dynamin-2 to promote GLUT4 endocytosis in muscle cells. *The Journal of Cell Biology.* 2023;222(2). doi:10.1083/jcb.202102119
74. Jiang A, Gormal R, Wallis T, et al. Dynamin1 long- and short-tail isoforms exploit distinct recruitment and spatial patterns to form endocytic nanoclusters. doi:10.21203/rs.3.rs-2641489/v1
75. Imoto Y, Raychaudhuri S, Ma Y, et al. Dynamin is primed at endocytic sites for ultrafast endocytosis. *Neuron.* 2022;110(17):2815-2835.e13. doi:10.1016/j.neuron.2022.06.010

76. Muhlberg AB. Domain structure and intramolecular regulation of dynamin GTPase. *The EMBO Journal*. 1997;16(22):6676-6683. doi:10.1093/emboj/16.22.6676
77. Sweitzer SM, Hinshaw JE. Dynamin undergoes a GTP-dependent conformational change causing vesiculation. *Cell*. 1998;93(6):1021-1029. doi:10.1016/S0092-8674(00)81207-6
78. Smirnova E, Shurland DL, Newman-Smith ED, Pishvaee B, Van Der Blik AM. A model for dynamin self-assembly based on binding between three different protein domains. *Journal of Biological Chemistry*. doi:10.1074/jbc.274.21.14942
79. Hinshaw JE. *DYNAMIN AND ITS ROLE IN MEMBRANE FISSION*. Vol 16.; 2000:483-519.
80. Dar S, Kamerkar SC, Pucadyil TJ. A high-throughput platform for real-time analysis of membrane fission reactions reveals dynamin function. *Nature Cell Biology*. 2015;17(12):1588-1596. doi:10.1038/ncb3254
81. Srinivasan S, Dharmarajan V, Reed DK, Griffin PR, Schmid SL. Identification and function of conformational dynamics in the multidomain GTPase dynamin. *The EMBO Journal*. 2016;35(4):443-457. doi:10.15252/embj.201593477
82. Hinshaw JE, Schmid SL. Dynamin self-assembles into rings suggesting a mechanism for coated vesicle budding. *Nature*. 1995;374(6518):190-192. doi:10.1038/374190a0
83. Kong L, Sochacki KA, Wang H, et al. Cryo-EM of the dynamin polymer assembled on lipid membrane. *Nature*. 2018;560(7717):258-262. doi:10.1038/s41586-018-0378-6
84. Marks B, Stowell MHB, Vallis Y, et al. GTPase activity of dynamin and resulting conformation change are essential for endocytosis. *Nature*. 2001;410(6825):231-235. doi:10.1038/35065645
85. Chappie JS, Acharya S, Leonard M, Schmid SL, Dyda F. G domain dimerization controls dynamin's assembly-stimulated GTPase activity. *Nature*. 2010;465(7297):435-440. doi:10.1038/nature09032
86. Morlot S, Roux A. Mechanics of Dynamin-Mediated Membrane Fission. *Annual Review of Biophysics*. 2013;42(1):629-649. doi:10.1146/annurev-biophys-050511-102247
87. Warnock DE, Schmid SL. Dynamin GTPase, a force generating molecular switch. *BioEssays*. 1996;18 (11).
88. Liu J, Alvarez FJD, Clare DK, Noel JK, Zhang P. CryoEM structure of the super-constricted two-start dynamin 1 filament. *Nat Commun*. 2021;12(1):5393. doi:10.1038/s41467-021-25741-x
89. Hinostroza F, Neely A, Araya-Duran I, et al. Dynamin-2 R465W mutation induces long range perturbation in highly ordered oligomeric structures. *Sci Rep*. 2020;10(1):18151. doi:10.1038/s41598-020-75216-0
90. Musacchio A, Gibson T, Rice P, Thompson J, Saraste M. The PH domain: a common piece in the structural pathwork of signalling proteins. *Trends in Biochemical Sciences*. 1993;18(9):343-348. doi:10.1016/0968-0004(93)90071-T

91. Lemmon MA, Ferguson KM, Schlessinger J. *PH Domains: Diverse Sequences with a Common Fold Recruit Signaling Molecules to the Cell Surface*. Vol 85.; 1996:621-624. Accessed August 9, 2019. <https://www.cell.com/action/showPdf?pii=S0092-8674%2800%2981022-3>
92. Rebecchi MJ, Scarlata S. PLECKSTRIN HOMOLOGY DOMAINS: A Common Fold with Diverse Functions. *Annual Review of Biophysics and Biomolecular Structure*. 1998;27(1):503-528. doi:10.1146/annurev.biophys.27.1.503
93. Ferguson KM, Lemmon MA, Schlessinger J, Sigler PB. Crystal structure at 2.2 Å resolution of the pleckstrin homology domain from human dynamin. *Cell*. 1994;79(2):199-209. doi:10.1016/0092-8674(94)90190-2
94. Khurana H, Baratam K, Bhattacharyya S, Srivastava A, Pucadyil TJ. Mechanistic analysis of a novel membrane-interacting variable loop in the pleckstrin-homology domain critical for dynamin function. *Proceedings of the National Academy of Sciences*. 2023;120(11):e2215250120. doi:10.1073/pnas.2215250120
95. Garcia P, Gupta R, Shah S, et al. *The Pleckstrin Homology Domain of Phospholipase C- $\Delta 1$ Binds with High Affinity to Phosphatidylinositol 4,5-Bisphosphate in Bilayer Membranes*. Vol 34.; 1995:16228-16234. doi:10.1021/bi00049a039
96. Lemmon MA, Ferguson KM, O'Brien R, Sigler PB, Schlessinger J. Specific and high-affinity binding of inositol phosphates to an isolated pleckstrin homology domain. *Proceedings of the National Academy of Sciences of the United States of America*. 1995;92(23):10472-10476. doi:10.1073/pnas.92.23.10472
97. Ferguson KM, Lemmon MA, Schlessinger J, Sigler PB. Structure of the high affinity complex of inositol trisphosphate with a phospholipase C pleckstrin homology domain. *Cell*. 1995;83(6):1037-1046. doi:10.1016/0092-8674(95)90219-8
98. Zheng J, Cahill SM, Lemmon MA, Fushman D, Schlessinger J, Cowburn D. Identification of the binding site for acidic phospholipids on the PH domain of dynamin: Implications for stimulation of GTPase activity. *Journal of Molecular Biology*. 1996;255(1):14-21. doi:10.1006/jmbi.1996.0002
99. Klein DE, Lee A, Frank DW, Marks MS, Lemmon MA. *The Pleckstrin Homology Domains of Dynamin Isoforms Require Oligomerization for High Affinity Phosphoinositide Binding*. Vol 273.; 1998:27725-27733. doi:10.1074/jbc.273.42.27725
100. Lemmon MA. Pleckstrin homology (PH) domains and phosphoinositides. *Biochemical Society Symposium*. 2007;74:81-93. doi:10.1042/bss2007c08
101. Mehrotra N, Nichols J, Ramachandran R. Alternate pleckstrin homology domain orientations regulate dynamin-catalyzed membrane fission. *Molecular Biology of the Cell*. 2014;25(6):879-890. doi:10.1091/mbc.e13-09-0548
102. Ramachandran R, Pucadyil TJ, Liu YW, et al. Membrane Insertion of the Pleckstrin Homology Domain Variable Loop 1 Is Critical for Dynamin-catalyzed Vesicle Scission. *MBoC*. 2009;20(22):4630-4639. doi:10.1091/mbc.e09-08-0683

103. Baratam K, Jha K, Srivastava A. Flexible pivoting of dynamin pleckstrin homology domain catalyzes fission: insights into molecular degrees of freedom. *Molecular Biology of the Cell*. 2021;32(14):1306-1319. doi:10.1091/mbc.e20-12-0794
104. Chin YH, Lee A, Kan HW, et al. Dynamin-2 mutations associated with centronuclear myopathy are hypermorphic and lead to T-tubule fragmentation. *Human Molecular Genetics*. 2015;24(19):5542-5554. doi:10.1093/hmg/ddv285
105. Tassin TC, Barylko B, Hedde PN, et al. Gain-of-Function Properties of a Dynamin 2 Mutant Implicated in Charcot-Marie-Tooth Disease. *Front Cell Neurosci*. 2021;15:745940. doi:10.3389/fncel.2021.745940
106. Pettersen EF, Goddard TD, Huang CC, et al. UCSF Chimera—A visualization system for exploratory research and analysis. *Journal of Computational Chemistry*. 2004;25(13):1605-1612. doi:10.1002/JCC.20084
107. Pettersen EF, Goddard TD, Huang CC, et al. UCSF ChimeraX: Structure visualization for researchers, educators, and developers. *Protein Science*. 2021;30(1):70-82. doi:10.1002/PRO.3943
108. Bethoney KA, King MC, Hinshaw JE, Ostap EM, Lemmon MA. A possible effector role for the pleckstrin homology (PH) domain of dynamin. *Proceedings of the National Academy of Sciences*. 2009;106(32):13359-13364. doi:10.1073/pnas.0906945106
109. Achiriloaie M, Barylko B, Albanesi JP. Essential Role of the Dynamin Pleckstrin Homology Domain in Receptor-Mediated Endocytosis. *Molecular and Cellular Biology*. 1999;19(2):1410-1415. doi:10.1128/mcb.19.2.1410
110. Taylor MJ, Perrais D, Merrifield CJ. A High Precision Survey of the Molecular Dynamics of Mammalian Clathrin-Mediated Endocytosis. *PLOS Biology*. 2011;9(3):e1000604. doi:10.1371/JOURNAL.PBIO.1000604
111. Dar S, Pucadyil TJ. The pleckstrin-homology domain of dynamin is dispensable for membrane constriction and fission. *Molecular Biology of the Cell*. 2016;28(1):152-160. doi:10.1091/mbc.e16-09-0640
112. Pucadyil TJ, Chipuk JE, Liu Y, O'Neill L, Chen Q. The multifaceted roles of mitochondria. *Molecular Cell*. 2023;83(6):819-823. doi:10.1016/j.molcel.2023.02.030
113. Züchner S, Nouredine M, Kennerson M, et al. Mutations in the pleckstrin homology domain of dynamin 2 cause dominant intermediate Charcot-Marie-Tooth disease. *Nature genetics*. 2005;37(3):289-294. doi:10.1038/NG1514
114. Durieux AC, Vignaud A, Prudhon B, et al. A centronuclear myopathy-dynamin 2 mutation impairs skeletal muscle structure and function in mice. *Human Molecular Genetics*. 2010;19(24):4820-4836. doi:10.1093/hmg/ddq413
115. Kenniston JA, Lemmon MA. Dynamin GTPase regulation is altered by PH domain mutations found in centronuclear myopathy patients. *The EMBO Journal*. 2010;29:3054-3067. doi:10.1038/emboj.2010.187

116. Haberlová J, Mazanec R, Ridzoň P, et al. Phenotypic variability in a large Czech family with a dynamin 2-associated Charcot-Marie-Tooth neuropathy. *Journal of Neurogenetics*. 2011;25(4):182-188. doi:10.3109/01677063.2011.627484
117. González-Jamett A, Momboisse F, Haro-Acuña V, Bevilacqua J, Caviedes P, Cárdenas A. Dynamin-2 Function and Dysfunction Along the Secretory Pathway. *Frontiers in Endocrinology*. 2013;4. Accessed September 14, 2023. <https://www.frontiersin.org/articles/10.3389/fendo.2013.00126>
118. Hohendahl A, Roux A, Galli V. Structural insights into the centronuclear myopathy-associated functions of BIN1 and dynamin 2. *Journal of structural biology*. 2016;196(1):37-47. doi:10.1016/J.JSB.2016.06.015
119. González-Jamett AM, Baez-Matus X, Olivares MJ, et al. Dynamin-2 mutations linked to Centronuclear Myopathy impair actin-dependent trafficking in muscle cells. *Sci Rep*. 2017;7(1):4580. doi:10.1038/s41598-017-04418-w
120. Lionello VM, Kretz C, Edelweiss E, et al. BIN1 modulation in vivo rescues dynamin-related myopathy. *Proc Natl Acad Sci U S A*. 2022;119(9):e2109576119. doi:10.1073/pnas.2109576119
121. Cowling BS, Toussaint A, Muller J, Laporte J. Defective Membrane Remodeling in Neuromuscular Diseases: Insights from Animal Models. *PLOS Genetics*. 2012;8(4):e1002595. doi:10.1371/journal.pgen.1002595
122. Jose GP, Gopan S, Bhattacharyya S, Pucadyil TJ. A facile, sensitive and quantitative membrane-binding assay for proteins. *Traffic*. 2020;21(3):297-305. doi:10.1111/tra.12719
123. Jose GP, Pucadyil TJ. PLiMAP : Proximity-Based Labeling of Membrane-Associated Proteins. *Current Protocols in Protein Science*. 2020;101:1-12. doi:10.1002/cpp.110
124. Baykov AA, Evtushenko OA, Avaeva SM. A malachite green procedure for orthophosphate determination and its use in alkaline phosphatase-based enzyme immunoassay. *Analytical biochemistry*. 1988;171(2):266-270.
125. Dar S, Kamerkar SC, Pucadyil TJ. Use of the supported membrane tube assay system for real-time analysis of membrane fission reactions. *Nature Protocols*. 2017;12(2):390-400. doi:10.1038/nprot.2016.173
126. Schindelin J, Arganda-Carreras I, Frise E, et al. Fiji: an open-source platform for biological-image analysis. *Nature Methods* 2012 9:7. 2012;9(7):676-682. doi:10.1038/nmeth.2019
127. Fuhrmans M, Müller M. Coarse-grained simulation of dynamin-mediated fission. *Soft Matter*. 2015;11(8):1464-1480. doi:10.1039/C4SM02533D
128. Hatzakis NS, Bhatia VK, Larsen J, et al. How curved membranes recruit amphipathic helices and protein anchoring motifs. *Nature chemical biology*. 2009;5(11):835-841. doi:10.1038/NCHEMBIO.213

129. Vanni S, Hirose H, Barelli H, Antonny B, Gautier R. A sub-nanometre view of how membrane curvature and composition modulate lipid packing and protein recruitment. *Nature communications*. 2014;5. doi:10.1038/NCOMMS5916
130. Mattila JP, Shnyrova AV, Sundborger AC, et al. A hemi-fission intermediate links two mechanistically distinct stages of membrane fission. *Nature*. 2015;524(7563):109-113. doi:10.1038/nature14509
131. Ramjaun AR, McPherson PS. Multiple Amphiphysin II Splice Variants Display Differential Clathrin Binding: Identification of Two Distinct Clathrin-Binding Sites. *Journal of Neurochemistry*. 1998;70(6):2369-2376. doi:10.1046/J.1471-4159.1998.70062369.X
132. Meinecke M, Boucrot E, Camdere G, Hon WC, Mittal R, McMahon HT. Cooperative Recruitment of Dynamin and BIN/Amphiphysin/Rvs (BAR) Domain-containing Proteins Leads to GTP-dependent Membrane Scission. *J Biol Chem*. 2013;288(9):6651-6661. doi:10.1074/jbc.M112.444869
133. Picas L, Viaud J, Schauer K, et al. BIN1/M-Amphiphysin2 induces clustering of phosphoinositides to recruit its downstream partner dynamin. *Nature Communications* 2014 5:1. 2014;5(1):1-12. doi:10.1038/ncomms6647
134. Adam J, Basnet N, Mizuno N. Structural insights into the cooperative remodeling of membranes by amphiphysin/BIN1. *Scientific reports*. 2015;5. doi:10.1038/SREP15452
135. Takei K, Slepnev VI, Haucke V, De Camilli P. Functional partnership between amphiphysin and dynamin in clathrin-mediated endocytosis. *Nat Cell Biol*. 1999;1(1):33-39. doi:10.1038/9004
136. Hohendahl A, Talledge N, Galli V, et al. Structural inhibition of dynamin-mediated membrane fission by endophilin. *eLife*. 2017;6. doi:10.7554/ELIFE.26856
137. Damke H, Baba T, Warnock DE, Schmid SL. Induction of mutant dynamin specifically blocks endocytic coated vesicle formation. *J Cell Biol*. 1994;127.
138. Ramachandran R, Surka M, Chappie JS, et al. The dynamin middle domain is critical for tetramerization and higher-order self-assembly. *EMBO Journal*. 2007;26(2):559-566. doi:10.1038/sj.emboj.7601491
139. Roux A, Koster G, Lenz M, et al. Membrane curvature controls dynamin polymerization. *Proceedings of the National Academy of Sciences*. 2010;107(9):4141-4146. doi:10.1073/pnas.0913734107
140. Salim K, Bottomley MJ, Querfurth E, et al. Distinct specificity in the recognition of phosphoinositides by the pleckstrin homology domains of dynamin and Bruton's tyrosine kinase. *The EMBO Journal*. 1996;15(22):6241-6250. doi:10.1002/j.1460-2075.1996.tb01014.x
